

Document downloaded from:

<http://hdl.handle.net/10251/150644>

This paper must be cited as:

Dhakshinamoorthy, A.; Asiri, A.; García Gómez, H. (2019). Formation of C-C and C-Heteroatom Bonds by C-H Activation by Metal Organic Frameworks as Catalysts or Supports. *ACS Catalysis*. 9(2):1081-1102. <https://doi.org/10.1021/acscatal.8b04506>



The final publication is available at

<https://doi.org/10.1021/acscatal.8b04506>

Copyright American Chemical Society

Additional Information

"This document is the Accepted Manuscript version of a Published Work that appeared in final form in *ACS Catalysis*, copyright © American Chemical Society after peer review and technical editing by the publisher. To access the final edited and published work see <https://doi.org/10.1021/acscatal.8b04506>"

Formation of C-C and C-Heteroatom bonds by C-H Activation by Metal Organic Frameworks as Catalysts or Supports

Amarajothi Dhakshinamoorthy,^{*a} Abdullah M. Asiri,^b Hermenegildo Garcia^{*c}

^aSchool of Chemistry, Madurai Kamaraj University, Madurai-625 021, Tamil Nadu, India. E-mail: admguru@gmail.com

^bCenter of Excellence for Materials Research, King Abdulaziz University, Jeddah, Saudi Arabia

^cDepartamento de Química and Instituto Universitario de Tecnología Química (CSIC-UPV), Av. De los Naranjos s/n, 46022 Valencia, Spain. E-mail: hgarcia@qim.upv.es

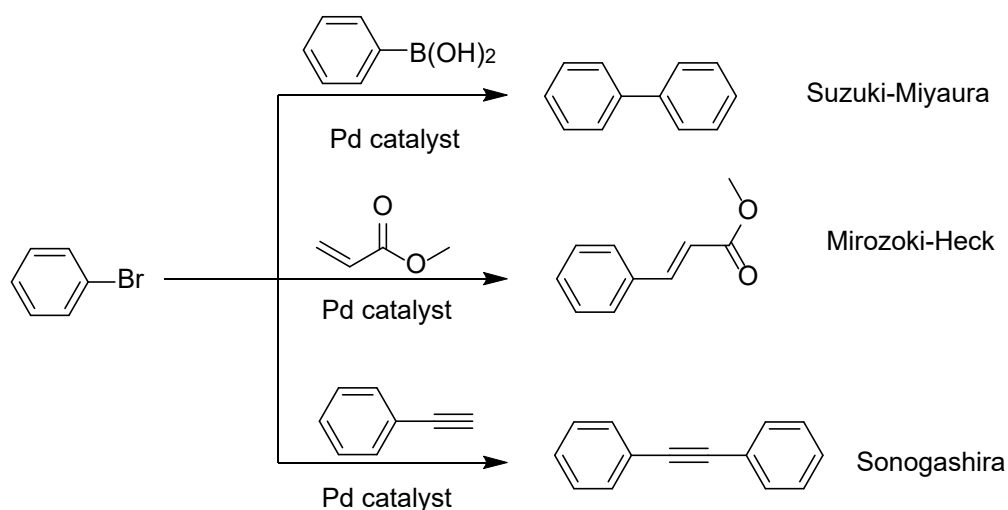
Abstract

Cross coupling reactions catalyzed by transition metals are currently among the most widely used transformations in organic synthesis. In most of these reactions, the coupling involves the reaction of two complementary functional groups, particularly boronates and halides. For the sake of atom economy and simplicity of the starting materials, it is more advantageous when the coupling involves C-H activation of one substrate lacking a reactive functional group. The present review focuses on the use of metal organic frameworks (MOFs) as solid reusable catalysts to promote cross-coupling reactions involving C-H activation. After general considerations, the review is organized according to the bond formed in the coupling, either C-C or C-heteroatom (N, O, B and X). The purpose of this mini review is to show the performance of MOFs as heterogeneous catalysts in these reactions, combining a high activity due to the large percentage of accessible metal sites and high stability allowing the reuse of the material in consecutive cycles. Comparison with homogeneous analogous catalysts indicates that this improved performance derives from the porosity, large surface area and site isolation and immobilization occurring in the MOFs. Considering the growing interests in these reactions the last section forecasts future developments in these areas in near future.

Keywords: Heterogeneous Catalysis; Metal Organic Frameworks; Cross-Coupling Reactions; C-H Activation; C-C Bond Formation; C-N Bond Formation; C-O Bond Formation; C-B Bond Formation.

1. Introduction

Modern organic synthesis has considerably progressed since the development of transition metal-catalyzed cross-coupling reactions, allowing for the easy formation of C-C and C-Y (Y: O, N, Si, X) among other bonds.¹⁻⁸ These cross-coupling reactions are generally carried out in the presence of minimal percentages of metal catalysts under mild conditions that are compatible with a large variety of functional groups. The reactions can take place affording high product yields and exhibiting wide substrate scope. Typical examples of cross-coupling reactions are Suzuki-Miyaura coupling^{3,4} to form biaryls by coupling of phenylboronic acids and aryl halides, Heck-Mirozoki reaction⁹ of aryl halides with activated C=C groups and Sonogashira coupling¹⁰ of terminal acetylenes with aryl halides, among other reactions (Scheme 1). In many cases, these coupling reactions involve two substrates having complementary functional groups that are removed in the coupling. Conventional strategies in traditional cross-coupling reactions use functionalized starting materials, like organic halides and organometallic reagents.



Scheme 1. Some conventional cross-coupling reactions catalyzed by Pd catalysts.

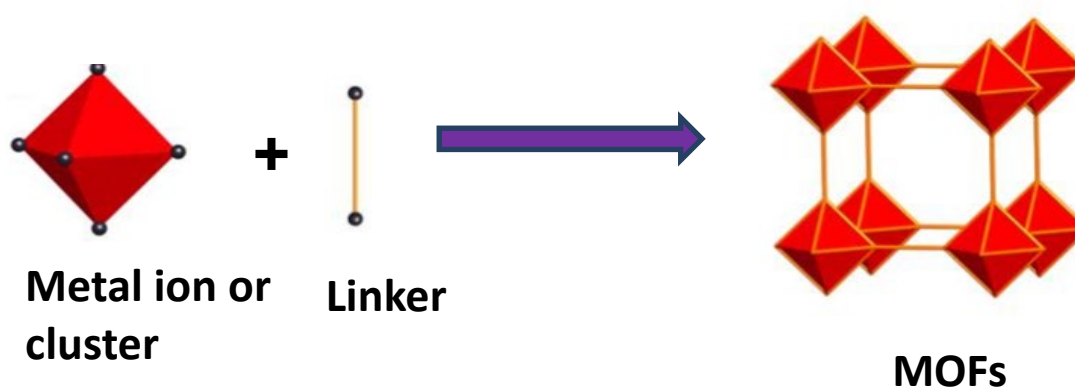
In recent years, considerable effort has been made to avoid either functionalized halides or organometallic reagents by developing suitable conditions and reagents that activate the C-H bond of the substrate at the coupling position. In this regard, one step forward in these coupling reactions is the use of substrates with C-H bond (either sp^2 or sp^3) as reactant in combination with another substrate that possesses a leaving group. Examples of these reactions are oxidative couplings of arenes with organometallic reagents catalyzed by Pd complexes¹¹ or radical C-H activation of substrates followed by cross coupling.¹²

Probably, the ideal method would involve coupling of two partners with C-H bonds that would undergo simultaneous activation, leading to C-C bond formation by the liberation of hydrogen, but such a hypothetical process still has to be developed as a general coupling process. At the moment, avoiding functionalization of just one of the two coupling substrates represents an improvement regarding atom economy, minimization of by-products and simplicity in synthesis design.

As indicated above, cross-coupling reactions require transition metal catalysis, Pd complexes being the most common catalysts. One logical evolution in catalysis is to transform a reaction requiring homogeneous soluble catalysts into an analogous process based on insoluble solids that can promote the reaction heterogeneously.¹³ By employing a catalyst in a separate phase, the active species can be easily recovered from the reaction mixture. This allows the design of continuous flow processes or the reuse of the catalyst in consecutive batch reactions.

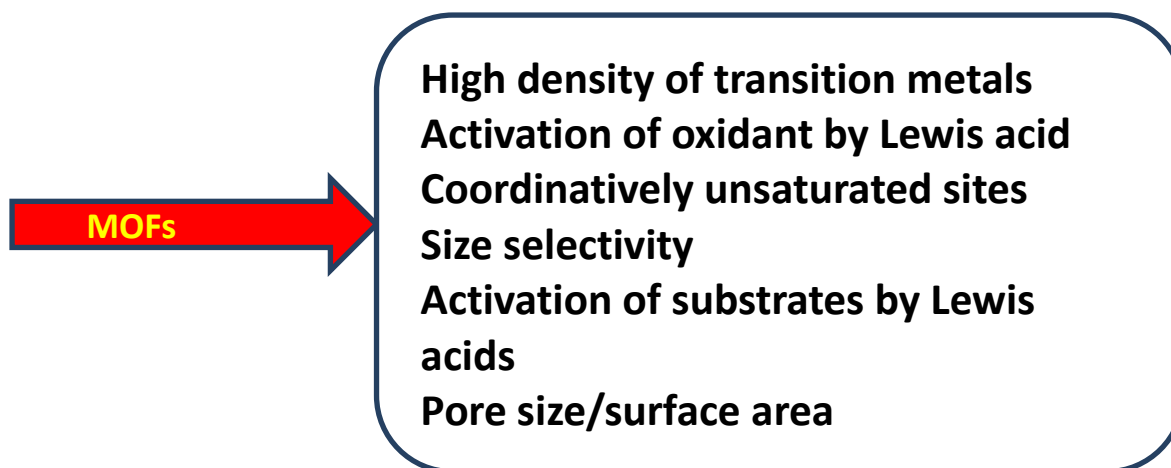
Of importance for the present review is the increasing use of metal organic frameworks (MOFs) as heterogeneous catalysts, particularly for liquid phase reactions.¹⁴⁻¹⁶ MOFs are

crystalline porous materials in where the structure is constructed by metallic nodes of a few atoms that are coordinated, generally through Columbic and coordinative bonds, with rigid bipodal or multipodal organic ligands.¹⁷⁻²¹ Among the most important properties of MOFs from the catalytic viewpoint, those related to porosity, high surface area and stability are the most important ones. Scheme 2 illustrates the structural building blocks and how the lattice is formed by the association of nodes and linkers.



Scheme 2. Structure and components of MOFs. Copyright 2014 American Chemical Society.²²

Due to a combination of composition and structural features, MOFs are considered among the most promising and versatile materials in heterogeneous catalysis under conditions compatible with their structure. Scheme 3 summarizes some of the positive properties that MOFs offer as heterogeneous catalysts, including high surface area, large pore volume and accessibility of a large density of active sites. Obviously, these properties are also important for the application of MOFs in cross-coupling reactions, particularly the presence of transition metals with oxidizing activity and Lewis acidity in a highly porous and accessible framework.



Scheme 3. Advantages offered by MOFs as heterogeneous catalysts, particularly for coupling reactions.

The large flexibility in the composition and diversity in the structure of the organic ligands determine the possibility to design MOFs for specific catalytic applications, such as C-H activation to promote coupling reactions.^{17, 22} In addition, besides the synthesis, MOFs can also be submitted to post-synthetic modifications^{23, 24} that allows to introduce, once the solid has been formed, additional metals in the composition of the material. One of the main advantages of MOFs is the large percentage of transition metal that can be present in the composition. In some cases, these transition metals complete some of their coordination sphere with ligands that are not involved in the structure of the material. In these cases, these ligands different from the linkers can be removed or exchanged by reagents and substrates. This situation is denoted indicating that the MOF contains *coordinatively unsaturated positions*.²⁵

In addition to the presence of coordinatively unsaturated positions in MOFs, it is becoming increasingly recognized that structural defects are playing a crucial role in catalysis.^{16, 26, 27} The current state of the art allows also to tune the density of defects by adding during the synthesis of the MOFs some modulating agent that controls the crystal growth.

These modulators can become reversibly attached to the metal nodes instead of the organic linker, disrupting in this way the crystal structure of the material.

This large transition metal content characteristic of MOFs, the large diversity of metals that can be used, together with the presence of coordinatively unsaturated positions in some cases or defects in others determine that MOFs exhibit in general a wide applicability as solid Lewis acids or as catalysts for oxidation reactions.^{28, 29} The present review is focused on the use of MOFs as heterogeneous catalysts to promote cross coupling reactions by C-H functionalization.

As it will be shown below, there are several pathways to promote cross coupling reactions by C-H activation. One possibility for C-C bond formation, C-H at α position to a nitrogen atom in aromatic heterocycles becomes activated. Typical examples are indoles or benzimidazoles. This activated α position can react, in the presence of MOFs as catalysts, with aryl halides, arylboronic and other reagents with leaving groups without the need of oxidizing reagent. However, in other cases in where no heteroatoms are present, sp^2 C-H bonds can also be activated to form C-C bonds through an oxidative mechanism that requires the presence of oxidizing reagents, sometimes in over stoichiometric amounts. In this reaction mechanism, the metal is playing a role of redox site and radical intermediates are generally involved. Other general C-H activation pathway for C-C bond formation is that involving acidic C-H bonds, the reaction occurring through conventional aldolic condensations. For this general reaction mechanism, MOFs are acting as solid Lewis acids. The advantages of all these process involving C-H activation are atom economy, wider availability of substrates without complementary functional group and the lack of formation of by-products arising from the leaving group.

While the above-commented three pathways of C-H activation can lead to the formation of C-C bonds, for generation of C-N, C-O, C-B and C-X bonds by C-H activation the presence of oxidants are needed. The most widely used oxidizing agent in C-X bond formation is tert-butylhydroperoxide (TBHP), although other reagents such as diphenyliodonium tetrafluoroborate, phenyl-N-tosyliodinane and oxygen can also be used. In this context, there is still a need of developing general oxidative cross-coupling reactions based on the use of molecular oxygen to activate these C-H bonds.

The main body of the present review is organized according to the type of bond that is formed in the coupling reaction. Due to their large application in organic synthesis and for the preparation of organic compounds with therapeutical properties, cross-coupling reactions leading to C-C and C-N bond formation using MOFs as catalysts represent the cases that have attracted more attention, particularly in comparison of the reported studies on C-O bond formation. Examples of these three reactions will be discussed in the following three sections.

Another part of this review deals with formation of C-B bonds. Since boronic acids and boronates have become important reagents for couplings, there is a considerable interest in establishing synthetic methods for the preparation of these important reagents. It will be shown below that in most of the cases, bis(pinacolato)diboron is the reagent of choice for the reactions developed so far. The last cross-coupling reaction presented will be the formation of C-X bond that constitutes an alternative to the use of halogens. The final section summarizes the review and forecasts future developments in this area.

The purpose of the present review is to show the current state of the art in the use of MOFs as heterogeneous catalysts for C-H activation leading to C-C and C-Y cross coupling reactions, showing the potential and advantages that these porous materials offer as catalysts for these types of reactions. When possible a comparison with the activity of homogeneous

catalysts will also be made. Table 1 summarizes the various MOFs used as heterogeneous solid catalysts or as supports for the formation of C-C, C-N, C-O, C-B and C-X bonds through the activation of sp^2/sp^3 C-H bonds. In addition, stability evidences of these MOFs have been also indicated.

Table 1. List of various MOFs used as solid catalysts or supports for the formation of C-C, C-N, C-O, C-B and C-X bonds.

Catalyst	Reaction category	Reaction	TON/TOF(h^{-1})	Stability evidence	Ref .
$Ni_2(BDC)_2(DABCO)$	C-C	C-H arylation of benzoxazoles	-	XRD, BET	30
$\{(H_3O)[Cu^I_2(CN)(TTB)_{0.5}]1.5H_2O\}_n$		C-H arylation of benzothiazole	-	XPS, ICP-AES, XRD	31
$Cu_2(BPDC)_2(BPY)$		C-H arylation of benzoxazole	-	XRD, FT-IR	32
$Pd@F15-NU-1000$		C-H arylation of indoles	-	XRD, TEM	33
$Pd/MIL-101(Cr)$		C-H arylation of N-methylindoles	-	XRD, BET	34
$Pd^{2+}@MOF-5(OH)$		C-H phenylation of naphthalene	-	TEM	35
$Fe_3(BTC)(NDC)_2 \cdot 6.65H_2O$ (VNU-20)		coupling of coumarin with N,N-dimethylaniline	-	XRD	36
$Fe_3O(BPDC)_3$		synthesis of 2-alkenylazaarenes	-	XRD, FT-IR	37

UiO-67-Pdbpydc _{0.5} /bpdc _{0.5}		Suzuki-Miyaura	-	ICP-OES, XRD	38
Pd(II) doped UiO-67		Suzuki-Miyaura and Heck	-	XRD, XPS	39
UiO-67-3-PI-Pd		Suzuki-Miyaura and Heck	1852 h ⁻¹	XPS, ICP-AES	40
MOF-199	C-N	coupling of N-benzoyl-8-amino-quinoline and morpholine	-	XRD	41
Cu-CPO-27		coupling of quinoxalin-2(1H)-one with morpholine	-	XRD, FT-IR	42
537-MOF		Synthesis of benzimidazoles	-	XRD	43
VNU-18		coupling of ethyl phenyl ketone and morpholine	-	leaching	44
Mn ₂₁ (TZBA) ₁₂ (HCO ₂) ₁₈ (H ₂ O) ₁₂ (CPF-5)		C-H amination of tetrahydrofuran	120000, 48000 h ⁻¹	XRD, ICP-MS	45
UiO-supported NacNac-Cu		C-H amination of cyclohexene	150	XRD, reuse	46
Cu ₂ (BPDC) ₂ (BPY)	C-O	Coupling of 2-hydroxybenzaldehyde and 1,4-dioxane	-	XRD, FT-IR	47
Fe ₂ (dobdc)		Activation of C-H bond in ethane	-	XRD, BET	48
mBPV-MOF-Ir	C-B	Borylation of m-xylene	17000	XRD, reuse	49

CoCl ₂ .TPY-MOL		C–H borylation of methylarenes	~ 40	XRD, ICP-MS	50
Pd@MIL-101-NH ₂ (Cr)	C-X	Halogenations of 2-phenylpyridine	-	XRD, TEM	51
UiO-Pd-TCAT		Halogenation of 2-phenylpyridine	-	reuse	52
PCN-602		Halogenation of cyclohexane	-	XRD, reuse	53

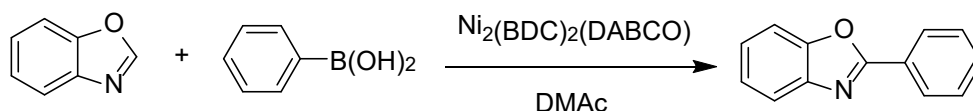
Abbreviations: BDC: 1,4-benzenedicarboxylic acid; DABCO: 1,4-diazacyclo[2.2.2]octane; H₄TTB: 1,2,4,5-tetra-(2H-tetrazole-5-yl)-benzene; BPDC: biphenyldicarboxylic acid; BPY: bipyridine; NDC: 2,6-naphthalenedicarboxylic acid; NacNac: β-Diketiminato; CPF: coordination porous framework; TZBA: 4-tetrazolate-benzoic acid; dobdc⁴: 2,5-dioxido-1,4-benzenedicarboxylate.

2. C-C Bond Formation

2.1 sp² C-H Activation

As indicated previously, there are three different cross-coupling mechanisms through which C-H can be activated to form C-C bonds. One of them requires the presence of a nitrogen atom at the α position. Thus, direct C-arylation of heterocycles using transition metals as homogeneous catalysts through activation of C-H bond has received considerable attention, since it does not require functionalization of the parent heterocycle.^{54, 55} In one of the recently reported examples, Ni₂(BDC)₂(DABCO) was prepared by solvothermal method and its crystal structure contains secondary building units (SBUs) of two 5-coordinate nickel cations as central metal ions bridged in a paddle wheel-type configuration as shown in Figure 1.⁵⁶ SEM images revealed the formation of crystalline solid while TEM images showed porous structure. Gas adsorption measurements indicated a median pore width of 6.1 Å with a BET surface area of around 1473 m²g⁻¹. Ni₂(BDC)₂(DABCO) exhibits catalytic activity in the direct C-H arylation of benzoxazoles and arylboronic acids to afford 2-arylbenzoxazoles (Scheme 4) at

100 °C in dimethylacetamide and K_3PO_4 as a base.³⁰ The obvious advantage of this reaction compared to the possible Suzuki-Miyaura coupling as alternative is that it does not require the use of the corresponding aryl halides as reagents. Interestingly, $Ni_2(BDC)_2(DABCO)$ showed significantly higher activity than other analogous Ni MOFs like $Ni_3(BTC)_2$ (BTC: 1,3,5-benzenetricarboxylate) and $Ni(BTC)(BPY)$ (BPY: 4,4'-bipyridine) under identical conditions. This difference in the activity between $Ni_2(BDC)_2(DABCO)$ and related MOFs may be due to their different structure imposing diffusion limitation to reach the metal centre. On other hand, the activity of $Ni_2(BDC)_2(DABCO)$ was also higher than homogeneous Ni^{2+} salts, such as $NiCl_2$, $Ni(NO_3)_2$, Ni_2SO_4 and $Ni(OAc)_2$ taken as reference for homogenous catalysts. The activity of $Ni_2(BDC)_2(DABCO)$ was maintained for seven cycles without significant activity loss. Powder XRD and pore size distribution measurements of the exhaustively used catalyst indicated that the crystallinity and pore volume were unaltered by its use as catalyst compared to the fresh material. The catalyst stability was further established by leaching experiments that support the heterogeneity of the process.



Scheme 4. Direct C-H arylation of benzoxazole with phenylboronic acid using $Ni_2(BDC)_2(DABCO)$ as solid catalyst.

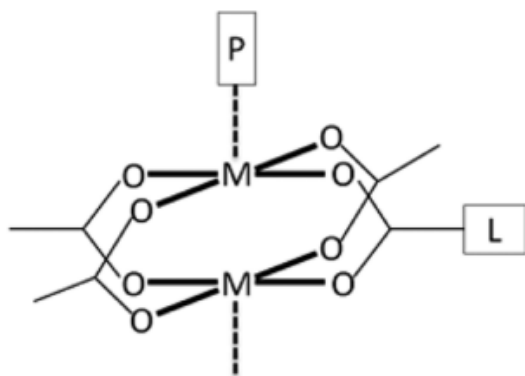
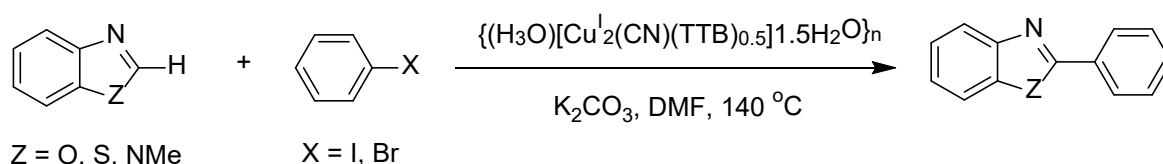
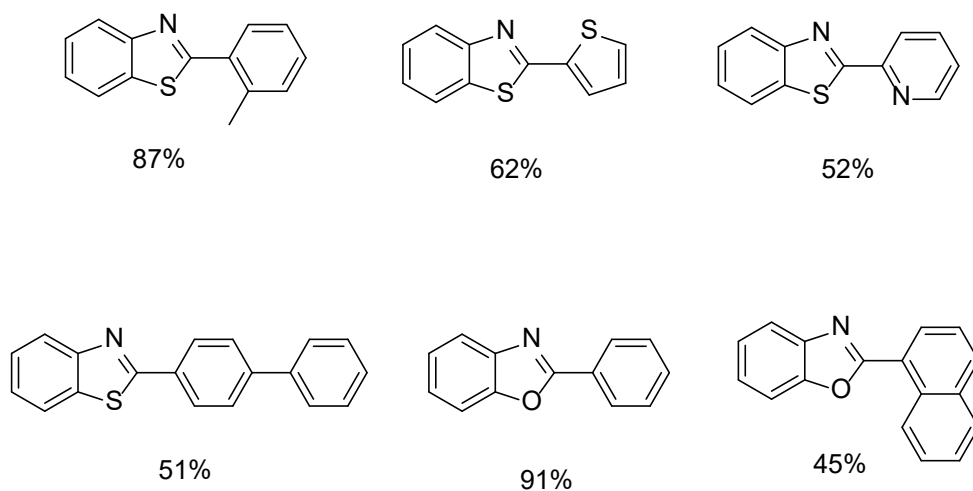


Figure 1. Illustration of the coordination geometry of paddle wheel building units in $\text{Ni}_2(\text{BDC})_2(\text{DABCO})$. M stands for metal ion, L stands for bicarboxylate linker (BDC) and P is N-containing bidentate pillar linker (DABCO). Reprinted with permission from ref. 56. Copyright 2012, American Chemical Society.

An anionic porous zeolite-like, three-dimensional MOF with molecular formula $\{(\text{H}_3\text{O})[\text{Cu}^{\text{I}}_2(\text{CN})(\text{TTB})_{0.5}]1.5\text{H}_2\text{O}\}_n$ was prepared containing free H_3O^+ ions as guest molecules.³¹ The catalytic performance of this Cu-MOF sample was evaluated in the C-H arylation of benzothiazole with iodobenzene through C-H activation (Scheme 5). Optimization of the reaction conditions leads to 90 % yield of the 2-phenylbenzothiazole using K_2CO_3 as the base in DMF at 140 °C. Interestingly, the crystallinity of $\{(\text{H}_3\text{O})[\text{Cu}^{\text{I}}_2(\text{CN})(\text{TTB})_{0.5}]1.5\text{H}_2\text{O}\}_n$ was retained during the course of the reaction. XPS analysis of the recovered sample did not reveal any change in the oxidation state of Cu. ICP-AES analysis indicated less than 0.1% of copper in the filtrate, thus, supporting the heterogeneity of the reaction. Although the yield slightly diminished during the reusability experiments, powder XRD of the five times reused sample did not show any sign of decomposition or collapse of MOF structure. Furthermore, this Cu MOF catalyst exhibits a wide scope, promoting the coupling of heteroarenes with a wide range of substituted aryl or heteroaryl halides to their respective heterocyclic derivatives in moderate to high yields (Scheme 6).



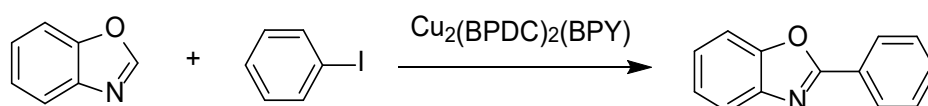
Scheme 5. The C-H arylation of azoles with iodobenzene using a Cu-MOF as solid catalyst.



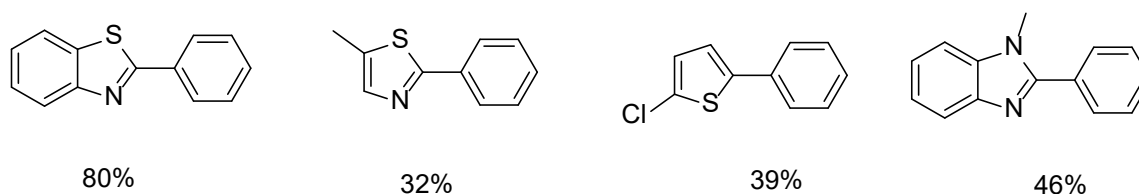
Scheme 6. Structure of heterocyclic compounds that can be obtained by C-H activation using $\{(H_3O)[Cu^I_2(CN)(TTB)_{0.5}]1.5H_2O\}_n$ catalyst.

In recent years, the synthesis of pillared layer, also called as ‘pillared-grid’, MOFs consisting bimetal paddle-wheel units (Figure 2) has attracted increasing attention.⁵⁷ The crystal structure of these types of MOFs reveals that dicarboxylates behave as grid-forming ligands and diamines or diimines acts as pillars, thus allowing the reactants to diffuse favourably to reach the active sites. In one of these examples, C-H arylation between benzoxazole and iodobenzene (Scheme 7) was reported using $Cu_2(BPDC)_2(BPY)$ as solid catalyst at 120 °C in DMSO and K_3PO_4 as the base, reaching complete conversion and selectivity.³² Control experiments with homogeneous copper salts indicated that the yield of the reaction is comparatively superior with heterogeneous MOF catalyst than with homogeneous copper catalysts. For instance, the coupling reaction in the presence of CuI afforded 80 % conversion, while CuCl provided 77 % conversion under similar experimental conditions. On the other hand, $CuCl_2$ showed even lower activity than the above salts by giving only 54 % conversion. Further, the catalytic activity of the $Cu_2(BPDC)_2(BPY)$ was compared with that of a series of analogous Cu-MOFs. Under identical reaction conditions, conversions of 79, 67, 11 and 45 % were reached using $Cu_3(BTC)_2$, $Cu(BDC)$, $Cu(BPDC)$, and

$\text{Cu}_2(\text{BDC})_2(\text{BPY})$ as catalysts, respectively. The distinctive catalytic behaviour between $\text{Cu}_2(\text{BPDC})_2(\text{BPY})$ and $\text{Cu}(\text{BPDC})$ suggests that the 4,4'-bipyridine linker is acting as a bridge to prevent diffusion limitation or the formation of catalytically inactive Cu-MOF.⁵⁸ The catalytic activity of $\text{Cu}_2(\text{BPDC})_2(\text{BPY})$ was retained for six cycles without noticeable decrease in activity. The reused catalyst exhibited identical absorption spectra and crystallinity as those of the fresh catalyst as evidenced by FT-IR spectroscopy and powder XRD analysis, respectively. The optimized reaction conditions using $\text{Cu}_2(\text{BPDC})_2(\text{BPY})$ as heterogeneous solid catalyst can be further exploited to obtain the series of heterocycles shown in Scheme 8.



Scheme 7. The C-H arylation of benzoxazole by iodobenzene promoted by $\text{Cu}_2(\text{BPDC})_2(\text{BPY})$ as solid catalyst.



Scheme 8. $\text{Cu}_2(\text{BPDC})_2(\text{BPY})$ catalyst mediated synthesis of wide range of heterocycles via C-H activation.

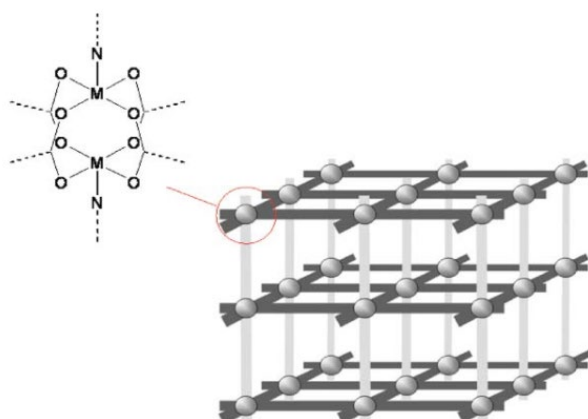


Figure 2. Pictorial representation of pillared-grid MOFs. Circles indicate bimetal paddlewheels, dark lines indicate grid-forming ligands (dicarboxylates) and lighter lines represent pillar ligands (diamines or diimines). Reprinted with permission from ref.57. Copyright 2007 Royal Society of Chemistry.

The structure of NU-1000 with the molecular formula of $Zr_6(\mu_3\text{-OH})_8(\text{OH})_8(\text{TBAPy})_2$ (TBAPy = 1,3,6,8-tetrakis(p-benzoate)pyrene)) consists in mesopores (3 nm) with considerably high thermal stability to around 500 °C, as well as chemical stability in boiling water. Interestingly, the available eight terminal OH groups on Zr nodes can be facilely modified by postmodification with perfluoroalkyl chains as shown in Figure 3. Later, ultrafine Pd nanoparticles (NPs) were encapsulated on hydrophobic perfluoroalkyl-functionalized mesoporous MOF NU-1000 (Fn-NU-1000; n= 9, 15 and 19). The activity of these fluorinated MOFs was examined in the C-H activation of indoles in water.³³ Pd NPs were embedded in NU-1000 and Fn-NU-1000 by incipient-wetness impregnation followed by reduction with hydrogen. The average particle size was around 2.5 nm which is compatible with the inclusion of Pd NPs within the mesopores of F15-NU-1000 MOF. The catalytic activity of the series of Pd NPs@Fn-NU-1000 was studied in the C-H arylation of indole by iodobenzene (Scheme 9) using potassium acetate at 100 °C in water. It was observed that the perfluoroalkyl functionalized NU-1000 promoted C-H activation more efficiently than the parent Pd@NU-1000. For instance, Pd@F9-NU-1000 afforded around two fold enhancement in the yield (24 %) than the Pd@NU-1000 (12.5 %) under identical conditions. Interestingly, Pd@F15-NU-1000 showed even higher activity (87.1 %) and selectivity than other tested catalysts. Further, Pd@F19-NU-1000 exhibited slightly lower activity (84.2 %) due to the lower surface area and pore volume of the MOF. Under the same conditions, Pd(acac)₂@F15-NU-1000 and Pd@MIL-101(Cr) catalysts showed of 11 and 33 % yields for the coupling product that indicates a much lower activity than Pd@F15-NU-1000. These activity data clearly show the importance of the

hydrophobicity of the internal pores of NU-1000 to enhance the activity. A series of indole derivatives were converted to their respective 2-phenylindoles with moderate to high yields under optimal reaction conditions. Hot filtration test was in agreement with the heterogeneity of the process. Pd@F15-NU-1000 was recycled for six runs in the C-H activation of N-methylindole and iodobenzene. The powder XRD patterns of the six-times recycled catalyst indicated maintenance of the crystallinity of MOF structure. Further, TEM images of the six-times recycled catalyst showed that the average Pd NP size is retained. Gas adsorption measurements also showed that there was no decrease in the surface area and pore volume after six recycles. Thus, all the available characterization data of the used catalyst indicates the stability of Pd@F15-NU-1000 under the reaction conditions.

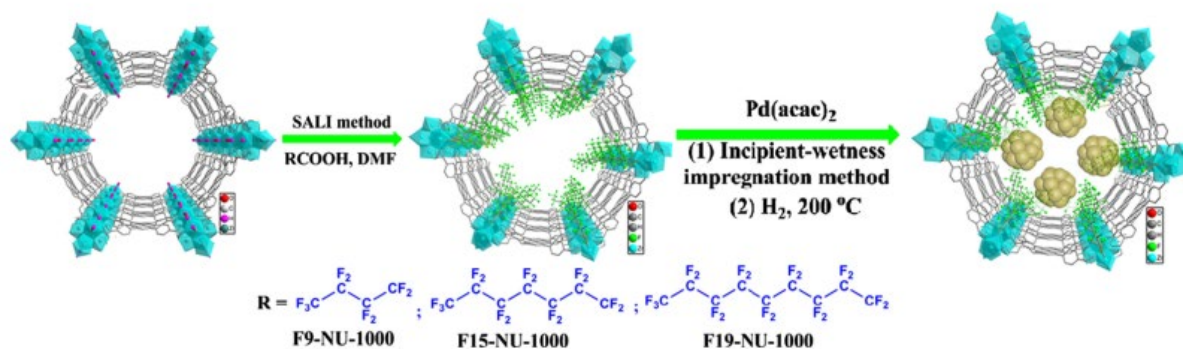
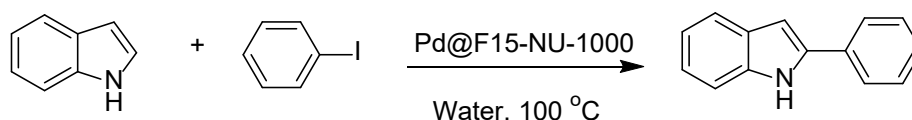


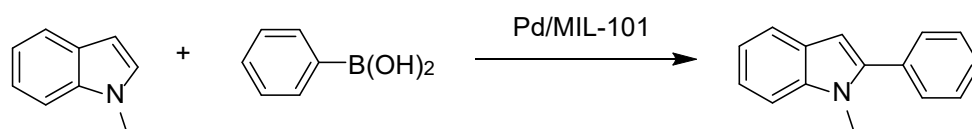
Figure 3. Schematic representation of introduction of perfluoroalkyl chains into the pores of NU-1000 by solvent-assisted ligand incorporation method followed by immobilization of the Pd NPs into the pores of perfluoroalkyl functionalized NU-1000 using incipient-wetness impregnation method. Reprinted with permission from ref.33 Copyright 2016 Elsevier.



Scheme 9. C-H activation of indole with iodobenzene catalyzed by Pd@F15-NU-1000 as catalyst in water.

MIL-101(Cr) was synthesised by Ferey and co-workers using Cr^{3+} as the metal ion and BDC as the linker, resulting in formation of highly crystalline structure with molecular formula as $\text{Cr}_3(\text{F},\text{OH})(\text{H}_2\text{O})_2\text{O}[\text{BDC}]_3 \cdot n\text{H}_2\text{O}$ ($n=25$).⁵⁹ The structure of MIL-101(Cr) exhibits extra large BET surface area ($3447 \text{ m}^2\text{g}^{-1}$) and two types of mesoporous cages (2.9 and 3.4 nm) accessible through microporous windows (1.2 and 1.4 nm). Highly dispersed Pd NPs with the mean diameter of $2.6 \pm 0.5 \text{ nm}$ were encapsulated over MIL-101(Cr) (Pd/MIL-101(Cr)) and their activity was tested in the C-H activation of N-methylindoles with arylboronic acids (Scheme 10) using oxygen or TEMPO as oxidant.³⁴ Optimization of the reaction conditions allowed to reach 98 % yield of 2-phenyl-N-methylindole for the coupling of N-methylindole with phenylboronic acid using Pd/MIL-101(Cr) as solid catalyst under aerobic conditions in dichloromethane/acetic acid medium at $60 \text{ }^\circ\text{C}$. In comparison, a control experiment with Pd/C catalyst (5 wt% Pd) gave only 19 % yield of the desired product under identical conditions. On the other hand, Pd/MIL-101(Cr)- NH_2 as catalyst showed a moderate activity of 51 % yield under the optimized conditions. The higher catalytic activity of Pd/MIL-101 compared to Pd/C and Pd/MIL-101- NH_2 was attributed to the larger specific surface area and accessible cages and windows of MIL-101, thus, favouring a high dispersion of Pd NPs and minimizing diffusion limitations. Furthermore, $\text{Pd}(\text{NO}_3)_2$ and $\text{Pd}(\text{OAc})_2$ adsorbed on MIL-101 also afforded much lower product yields of 9 and 16 %, respectively, to the coupling product under same conditions. These results are in line with the requirement of Pd NPs rather than isolated Pd^{2+} ions to promote this reaction. The catalytic reaction was heterogeneous and the leached Pd content was 0.9 ppm. Pd/MIL-101(Cr) was reused six cycles with no decay in its activity. Powder XRD and gas adsorption measurements showed no changes in the crystallinity and pore volume of MIL-101(Cr), respectively, after six cycles. In addition, Pd/MIL-101(Cr) exhibited wide substrate scope converting a series of indole derivatives containing electron

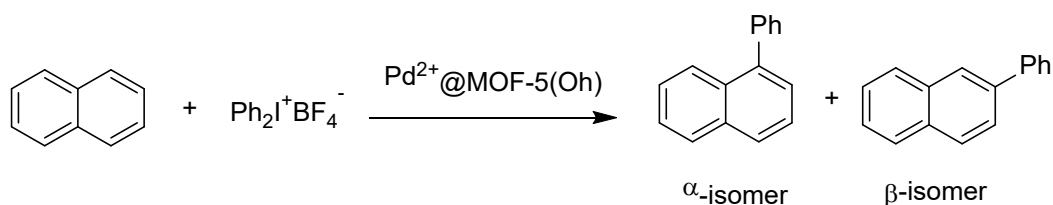
donating and withdrawing substituents to their respective 2-phenylindole derivatives in moderate to high yields.



Scheme 10. Pd/MIL-101 catalyzed C-H activation of N-methylindole with phenylboronic acid.

Besides activation of heterocycles at α -position of the nitrogen atom, other type of C(sp²)-H activation of aromatics requiring the assistance of oxidizing reagents has also been reported. In these cases, oxidative reaction conditions are required to promote the C-C coupling. One of these examples is the phenylation of naphthalene by diphenyliodonium tetrafluoroborate. A crystalline MOF-5(OH) was prepared with similar structure as that of MOF-5 by the reaction of Zn²⁺ with BDC in the presence of a certain proportion of 1,3,5-tris(4-carboxyphenyl)benzene (H₃BTB) (Figure 4). The structure of MOF-5 is constituted by the coordination between Zn²⁺ clusters with BDC ligands. In the case of MOF-5(OH), the presence of BTB originates a number of defective sites consisting in the presence of dangling carboxylates that can be used to anchor metal cations.³⁵ After its synthesis, MOF-5(OH) was treated with Pd(OAc)₂ to obtain a Pd²⁺@MOF-5(OH) solid. It is assumed that in Pd²⁺@MOF-5(OH) the Pd²⁺ ions are associated to the dangling carboxylate groups introduced by BTB. The activity of Pd²⁺@MOF-5(OH) was tested in the phenylation of naphthalene through C-H activation using diphenyliodonium tetrafluoroborate (Scheme 11). C-H arylation of naphthalene can be performed using Pd(OAc)₂ as homogeneous catalyst in nitrobenzene at 120 °C, affording a total yield of 13 % phenylnaphthalene with 15:1 selectivity for the α isomer over the β isomer after 30 min. The yield slightly increased (17 %) but the selectivity (α : β = 8:1) lowered after 17 h. On the contrary, the phenylation of naphthalene in the presence of Pd²⁺@MOF-5(OH) was significantly improved to 64 % after 12 h. Interestingly, Pd²⁺@MOF-

5(OH) catalyst exhibited different regioselectivity ($\alpha:\beta = 3:1$) compared to homogeneous Pd(OAc)₂ reaction. These activity data clearly show the superior performance of MOF catalyst by enhancing the yield, preserving the active sites and controlling the selectivity in a greater extent than the homogeneous Pd²⁺ salts. Hot-filtration test confirmed the heterogeneity of the reaction in the case of Pd@MOF-5(OH). TEM analysis of the recovered solid indicated the presence of relatively large Pd NPs of around 20 nm. Considering the large Pd NP size, these results still allow the design of more robust MOFs that could exhibit better C-H arylation yields and selectivity, while being stable under the reaction conditions.



Scheme 11. Pd²⁺@MOF-5(OH) catalyzed oxidative phenylation of naphthalene using diphenyliodonium tetrafluoroborate.

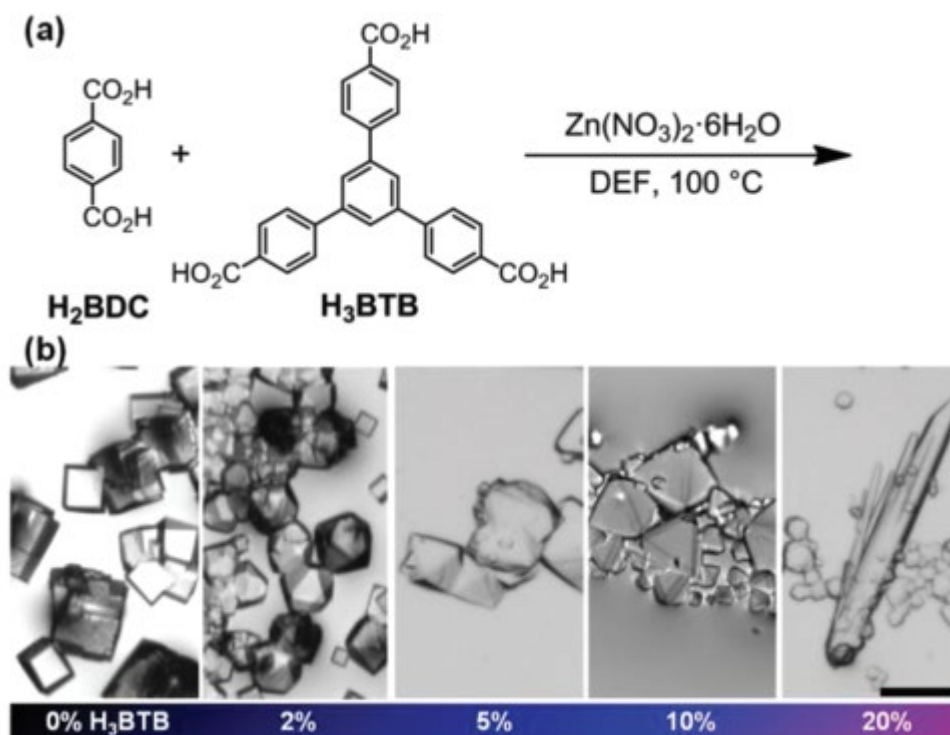
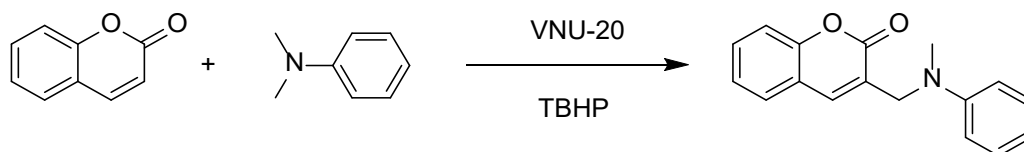


Figure 4. (a) Synthesis of BTB-incorporated MOF-5 crystals by addition of BTB to the reaction mixture of BDC and $\text{Zn}(\text{NO}_3)_2 \cdot 6\text{H}_2\text{O}$ (b) Photographs of crystals showing the dependence of the morphology upon the percentage of BTB in the feed (scale bar is 100 μm). Reprinted with permission from ref.35 Copyright 2011 American Chemical Society.

Recently, mixed-linker iron-based MOF, namely, VNU-20 with the molecular formula $\text{Fe}_3(\text{BTC})(\text{NDC})_2 \cdot 6.65\text{H}_2\text{O}$ has been synthesized. The structure of VNU-20 is constituted from the mixed linkers of BTC and NDC connecting the sinusoidal $[\text{Fe}_3(\text{CO}_2)_7]_\infty$ iron-rod secondary building units (Figure 5). These sinusoidal rods are linked by BTC^{3-} to expand horizontally. Further, these layers are pillared vertically by NDC^{2-} linkers to obtain three-dimensional VNU-20 (Figure 5). The structure consists of open rectangular window of $6.0 \times 8.7 \text{ \AA}^2$ and a BET surface area of $680 \text{ m}^2\text{g}^{-1}$. The activity of $\text{Fe}_3(\text{BTC})(\text{NDC})_2 \cdot 6.65\text{H}_2\text{O}$ was investigated for the coupling of coumarin with N,N-dimethylaniline through oxidative C-H bond activation³⁶ (Scheme 12). A yield of 94 % to the corresponding product was achieved at 120 °C using TBHP as oxidant and DABCO as cocatalyst. A series of control experiments firmly established that the oxidative C-C coupling requires the assistance of TBHP as oxidant, temperature about 120 °C and the use of DABCO. Homogeneous catalysts afforded moderate product yields, while heterogeneous catalysts like $\text{Fe}(\text{BTC})$ (80 %), $\text{Fe}_3\text{O}(\text{BDC})_3$ (62 %) and $\text{Fe}_3\text{O}(\text{BPDC})_3$ (82 %) exhibited comparable yields as VNU-20 under identical conditions. These catalytic data clearly illustrate the active role played by Fe^{3+} as Lewis acid sites activating TBHP. As shown in Figure 6, hydrogen was abstracted from N,N'-dimethylaniline by TBHP to give respective radical which was stabilized in the form of iminium. Later, this radical attacks to coumarin and gives a stable benzylic radical that later release a proton to form the desired final product by regenerating Fe(III) species in VNU-20. This proposal was further supported by homogeneous catalysts. Reusability tests indicated the stability of VNU-20 as it can be conveniently used for five cycles with no noticeable decay in its activity. Furthermore, VNU-20 exhibits a wide

substrate scope, since a series of coumarins can be readily coupled with *N,N*-dimethylanilines to obtain the desired products in high yields.



Scheme 12. VNU-20 catalyzed coupling of coumarin with *N,N*-dimethylaniline using TBHP as oxidant.

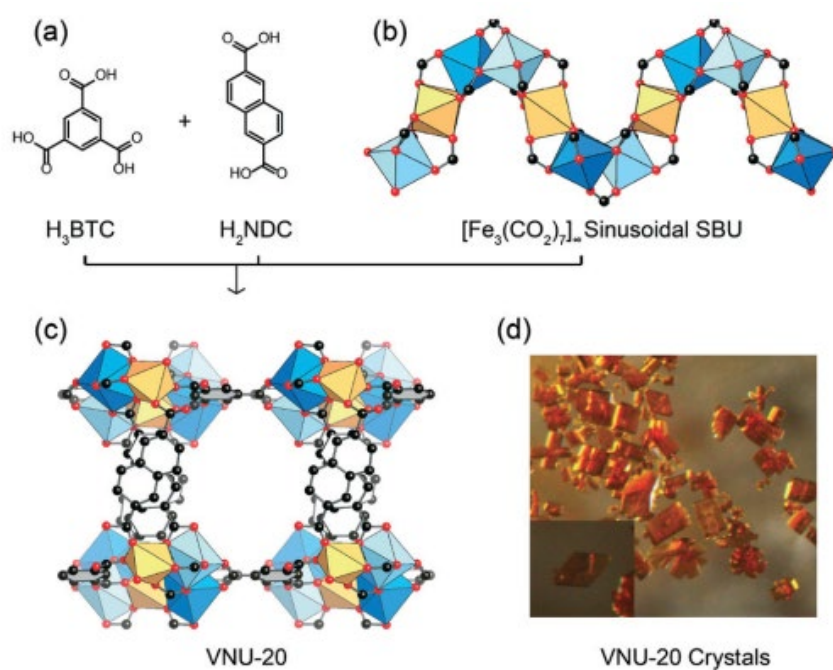


Figure 5. (a) Linker structures and (b) secondary building unit of VNU-20, (c) crystal structure of VNU-20 and (d) SEM image of VNU-20 crystals. Reprinted with permission from ref.36 Copyright 2018 Royal Society of Chemistry.

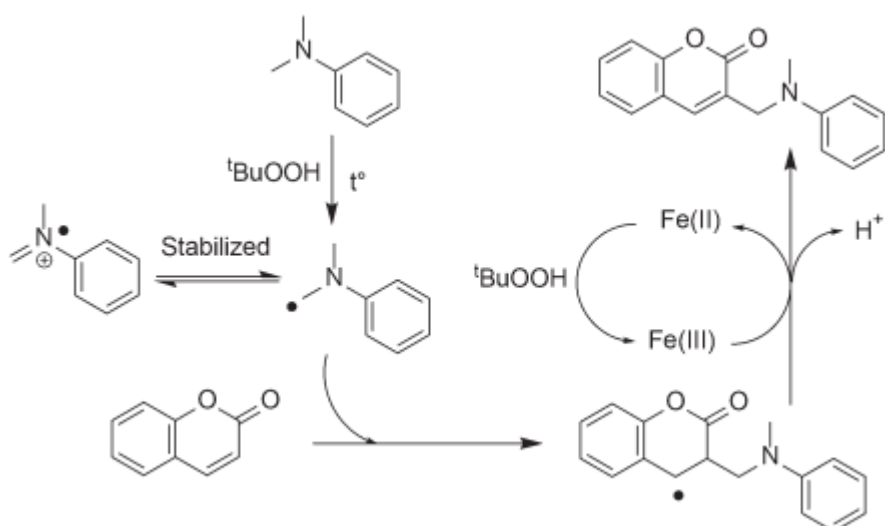


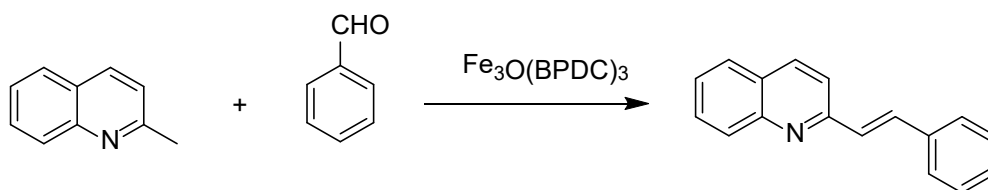
Figure 6. A proposed reaction mechanism for the coupling of N,N'-dimethylaniline with coumarin by VNU-20. Reprinted with permission from ref.36 Copyright 2018 Royal Society of Chemistry.

2.2 sp³ C-H Activation

In a different type of C-C coupling based on nucleophilic attack to carbonyl groups, Lewis acid sites at the metal nodes can act as catalytic sites. In one of the reported examples, a porous iron MOF with molecular formula of Fe₃O(BPDC)₃ was prepared by the reaction between iron(III) chloride hexahydrate and biphenyl-4,4'-dicarboxylic acid. Fe₃O(BPDC)₃ exhibits a rigid solid structure with an accessible three-dimensional pore system having BET surface area of around 1700 m²g⁻¹ (Figure 7).⁶⁰ Furthermore, infrared spectroscopy revealed the existence of coordinatively unsaturated Fe sites in the oxidation states of +2 and +3 by using NO and acetonitrile as probe molecules. The catalytic performance of Fe₃O(BPDC)₃ was tested in the synthesis of 2-alkenylazaarenes via condensation of 2-alkyl substituted azaarenes with carbonyl compounds through C-H bond activation (Scheme 13) in toluene at 120 °C under argon atmosphere.³⁷ Using Fe₃O(BPDC)₃ as catalyst a yield of (E)-2-styrylquinoline of 75 % was obtained, while a related Fe MOF with BDC ligands, Fe₃O(BDC)₃, afforded 50 % yield

under identical conditions. The enhanced activity observed for $\text{Fe}_3\text{O}(\text{BPDC})_3$ as catalyst may be due to its higher surface area and larger pore windows (0.7 nm) compared to $\text{Fe}_3\text{O}(\text{BDC})_3$ (0.4 nm). The study was completed by including other MOFs of different metals. Thus, the catalytic reaction with $\text{Cu}_2(\text{BDC})_2(\text{DABCO})$ provided 49 % yield of (E)-2-styrylquinoline, whereas $\text{Cu}_2(\text{NDC})_2(\text{DABCO})$ solid afforded 34 % yield under identical conditions. Although Zn-MOF-74 exhibited identical activity to $\text{Fe}_3\text{O}(\text{BDC})_3$ by giving 50 % yield, the use of $\text{Ni}_2(\text{BDC})_2(\text{DABCO})$ showed only 22 % of (E)-2-styrylquinoline. These data clearly infer that this reaction is highly dependent on the nature of metal ion as well as the structure of the MOFs, presumably due to the influence of surface area and pore volume.

This proposal was further confirmed by performing a control experiment with homogeneous FeCl_3 and observing 45 % yield of (E)-2-styrylquinoline under similar conditions. These catalytic data are compatible with the involvement of Fe^{3+} acting as a Lewis acid catalyst. Further, the catalytic activity of pyridine soaked $\text{Fe}_3\text{O}(\text{BPDC})_3$ was significantly reduced to around 40 % yield, supporting the role of Lewis acidity in promoting this reaction. Heterogeneity test confirmed that there was no contribution of leached iron species that could be present in the reaction mixture. The catalyst was still active up to the 7th cycle. Powder XRD and FT-IR spectra of the reused solid did not reveal changes, either in the crystallinity or IR spectra, compared to those of the fresh solid, thus, showing the stability under these experimental conditions. Regarding catalyst scope, $\text{Fe}_3\text{O}(\text{BPDC})_3$ was employed as solid catalyst to prepare a series of styrylquinolines in moderate to high yields.



Scheme 13. $\text{Fe}_3\text{O}(\text{BPDC})_3$ promoted coupling of 2-methylquinoline and benzaldehyde to form styrylquinoline.

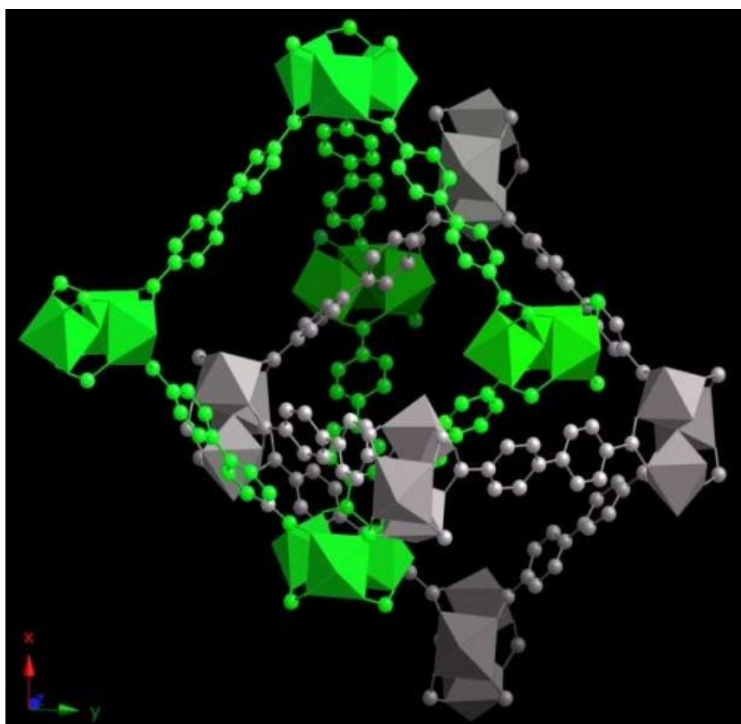
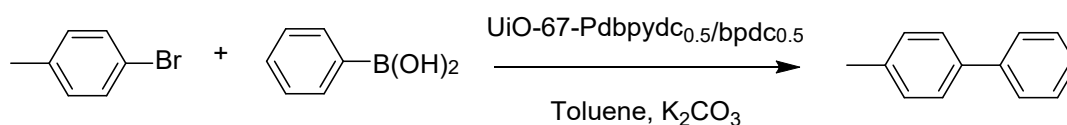


Figure 7. Organization of the two orthogonally interpenetrated trigonal bipyramidal building units in the crystal structure of $\text{Fe}_3\text{O}(\text{BPDC})_3$. Reprinted with permission from ref. 60 Copyright 2012 American Chemical Society.

2.3 Suzuki-Miyaura and Heck Cross-Coupling Reactions

As commented earlier in the introduction, Suzuki-Miyaura and Heck cross-coupling reactions are very often employed as general C-C bond forming reactions⁶¹ using MOFs as solid catalysts.^{62, 63} Hence, the reader is referred to the existing reviews for more detailed description on the use of MOFs as heterogeneous catalysts for these types of reactions.^{16, 64} However, some of the selected examples of these types of reactions are discussed below to demonstrate the tunability of MOFs to promote these reactions effectively. In one of these examples, two different approaches were reported to prepare a highly crystalline UiO-67-bpydc with open 2,2'-bipyridine chelating centres. UiO-67-bpydc was subsequently treated with

PdCl₂ to achieve highly active and recyclable Pd catalyst promoting Suzuki–Miyaura cross-coupling reaction (Figure 8).³⁸ Powder XRD of these MOFs indicated their isoreticular nature and high crystallinity. Furthermore SEM analysis showed that UiO-67-bpydc_x/bpdc_{1-x} materials have a uniform morphology with a crystal size around 1 μm. BET surface area values for UiO-67-bpydc_{0.5}/bpdc_{0.5} (containing 50 % bpydc, 2346±134 m²g⁻¹) and UiO-67-bpydc (containing 100 % bpydc, 2051±102 m²g⁻¹) were comparable to that of UiO-67 (2299±54 m²g⁻¹). These results indicate that UiO-67 does not lose its structural integrity during the linker exchange process. The Suzuki-Miyaura cross-coupling reaction between phenylboronic acid and 4-bromotoluene (Scheme 14) using UiO-67-Pdbpydc_{0.5}/bpdc_{0.5} as solid catalyst afforded 89 % yield of 4-phenyltoluene at 95 °C. In contrast, the pristine UiO-67 and UiO-67-bpydc_{0.5}/bpdc_{0.5} (without Pd metal) showed no product formation. Furthermore, controls using PdCl₂ and Pd(OAc)₂ as homogeneous catalysts resulted in lower yields (51–54 %) under identical conditions. A comparatively lower yield of 63 % was observed with a commercial 10 % Pd/C catalyst. ICP-OES analysis indicated less than 0.1 ppm Pd and less than 0.1 ppm Zr leaching in the reaction solution, thus supporting the superior stability of UiO-67-Pdbpydc_{0.5}/bpdc_{0.5} compared to Pd/C. UiO-67-Pdbpydc_{0.5}/bpdc_{0.5} catalyst retained its activity after three cycles. Powder XRD and SEM of UiO-67-Pdbpydc_{0.5}/bpdc_{0.5} indicated high crystallinity of the MOF sample used as catalysis compared to fresh material, thus highlighting the robust UiO structure.



Scheme 14. UiO-67-Pdbpydc_{0.5}/bpdc_{0.5} catalyzed Suzuki-Miyaura cross-coupling reaction.

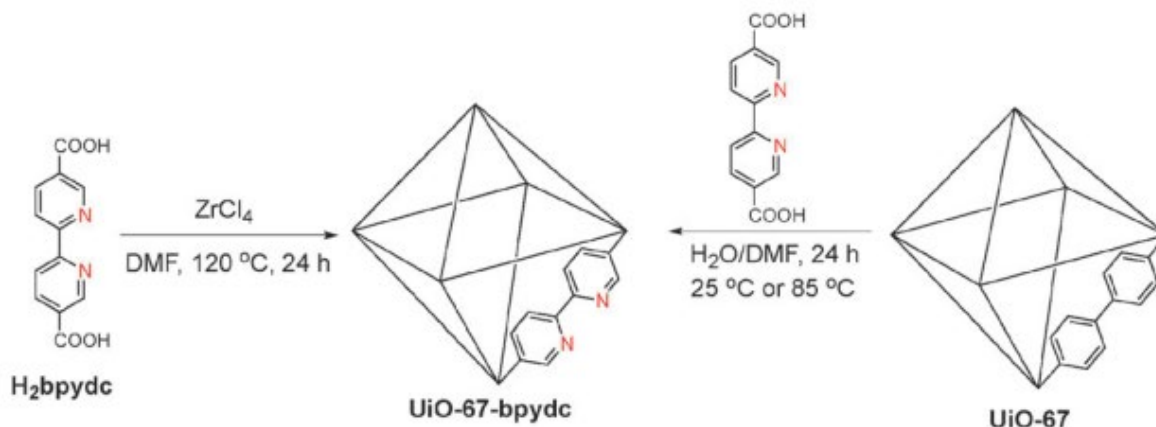


Figure 8. Preparation of UiO-67-bpydc either by direct synthesis or postsynthetic exchange method. Reprinted with permission from ref.38 Copyright 2014 Royal Society of Chemistry.

In another precedent, a mixed-ligand strategy was adopted to prepare UiO-67 MOF containing isolated Pd²⁺ active sites in a homogeneous distribution. This material was used to promote efficient C-C forming reactions through Suzuki-Miyaura and Heck cross-coupling reactions (Figure 9).³⁹ Pd(II) doped UiO-67 was isostructural to its parent UiO-67 framework with a BET surface area around 2000 m²g⁻¹ and a pore volume of 0.79 cm³g⁻¹. XPS analysis revealed the existence of divalent Pd(II) in doped UiO-67. Among the various reaction conditions screened for the Heck reaction between 4-chloroacetophenone and styrene (Scheme 15), a maximum of 99 % conversion of 4-chloroacetophenone with more than 99 % selectivity to 4-aceto-1,1'-biphenyl was achieved at 100 °C. On other hand, parent UiO-67 did not show any conversion under identical conditions, suggesting that the catalytic activity is derived from the ligand doped with Pd grafted to the UiO-67 structure. The wide substrate scope of Pd(II) doped UiO-67 was investigated by employing different aryl chlorides having various substituents with styrene and observing more than 85 % yields under identical conditions. In particular, 2-chloropyridine was successfully coupled with styrene to produce the desired product in 90 % yield. The Pd(II)-doped UiO-67 was reused for five cycles with no decay in its yield. Powder XRD patterns of the five times used catalyst showed identical pattern as the

fresh catalyst indicating the robust structure of UiO-67 under catalytic conditions. XPS measurements of the reused solid confirmed the presence of palladium in divalent state. Furthermore, Pd(II)-doped UiO-67 was also effective in promoting the Suzuki-Miyaura cross-coupling reaction of 4-nitrochlorobenzene and phenylboronic acid (Scheme 15) using K_2CO_3 in a DMF-EtOH mixture affording 97 % yield of the desired product. Under identical conditions, Pd(II)-doped UiO-67 promoted the cross-coupling reaction between different aryl chlorides with phenylboronic acid to afford the corresponding cross-coupling products in 80-97 % yields.

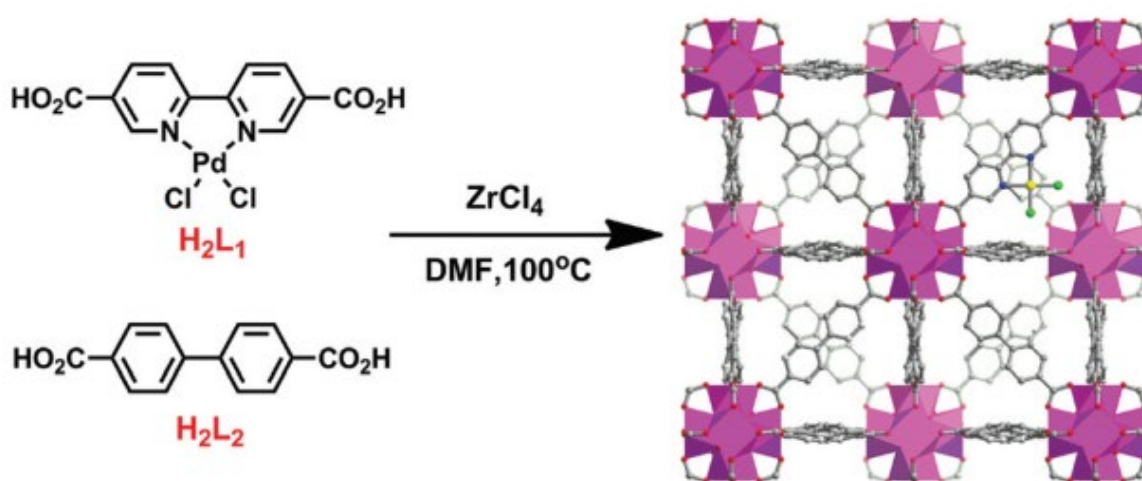
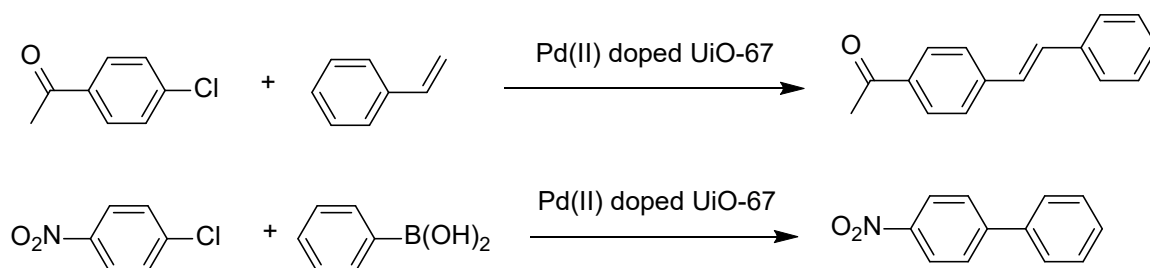


Figure 9. Synthesis of Pd(II)-doped UiO-67. The structure model (right) of Pd(II)-doped UiO-67 shows the incorporation of the L1 ligand into the framework. Reprinted with permission from ref. 39 Copyright 2014 Royal Society of Chemistry.



Scheme 15. Pd(II)-doped UiO-67 promoted Heck and Suzuki-Miyaura cross-coupling reactions.

Amine-functionalized Zr-based mixed-linker MOFs, namely, UiO-66-Mix and UiO-67-Mix were synthesized and subsequently the free amino groups were post-synthetically modified by reacting with pyridine-2-carboxaldehyde. Later, these pyridylimine moieties in the MOF strut were used as ligands to anchor Pd metal centers (Figure 10).⁴⁰ The activity of UiO-66-Mix-PI-Pd and UiO-67-Mix-PI-Pd in the Heck and Suzuki-Miyaura cross-coupling reactions were investigated. In general, the activity of UiO-66-Mix-PI-Pd was slightly lower than UiO-67-Mix-PI-Pd for both Suzuki-Miyaura and Heck cross-coupling reactions. For instance, UiO-66-3-PI-Pd afforded 78 and 61 % conversion of bromobenzene in the Suzuki-Miyaura and Heck coupling reactions, respectively. In contrast, UiO-67-3-PI-Pd showed 95 and 93 % conversions of bromobenzene for Suzuki-Miyaura and Heck coupling reactions, respectively, under identical conditions. Among the various reaction conditions screened, UiO-67-3-PI-Pd (0.054 mol %) afforded a TOF value of 1852 h⁻¹ for the reaction between iodobenzene and phenylboronic acid (Scheme 16). Similarly, UiO-67-3-PI-Pd (0.054 mol %) exhibited a TOF value of 1852 h⁻¹ for the reaction between iodobenzene and styrene (Scheme 16). Furthermore, UiO-67-3-PI-Pd was utilized to prepare wide range of biphenyl and stilbene derivatives containing electron donating and electron withdrawing substituents with more than 90 % yields. The catalytic reaction was heterogeneous in both cases as evidenced by hot-filtration test. Furthermore, ICP-AES analysis showed no presence of Pd in the reaction mixture. The UiO-67-3-PI-Pd catalyst was reused for ten cycles without significant decay in its activity. In addition, XPS of the recovered UiO-67-3-PI-Pd indicated the existence of Pd in the divalent state which further confirms the robust nature of this catalyst for ten successive cycles under the conditions required for the C-C coupling reactions.

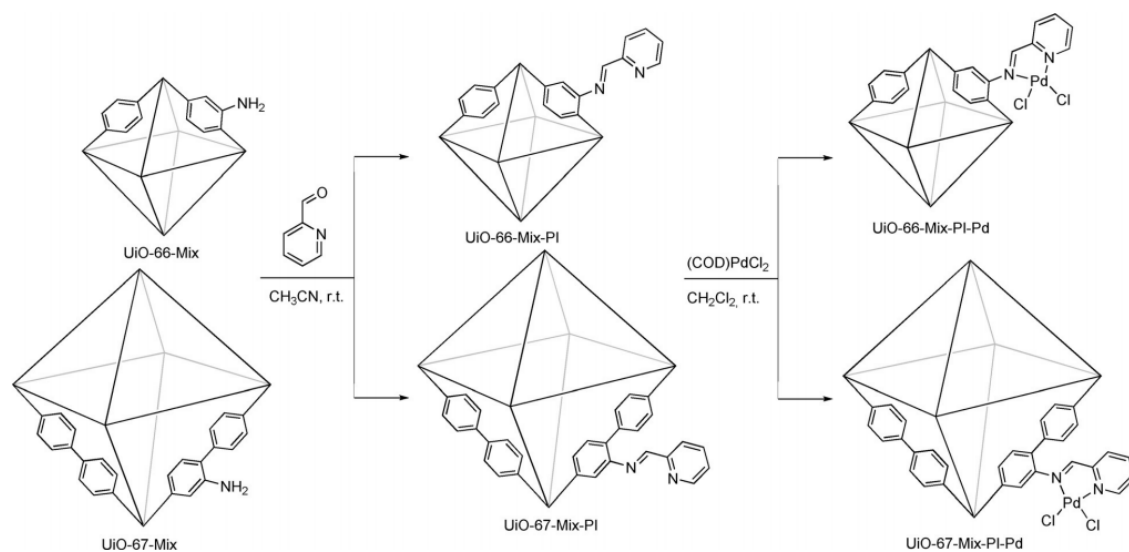
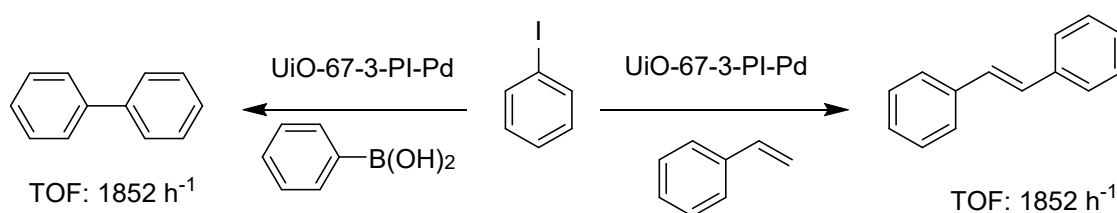


Figure 10. Post-synthetic modification of UiO-66-Mix and UiO-67-Mix to obtain UiO-66-Mix-PI-Pd and UiO-67-Mix-PI-Pd, respectively. Reprinted with permission from ref. 40 Copyright 2016 Wiley.



Scheme 16. UiO-67-3-PI-Pd catalyzed Heck and Suzuki-Miyaura cross-coupling reactions.

3. C-N bond formation

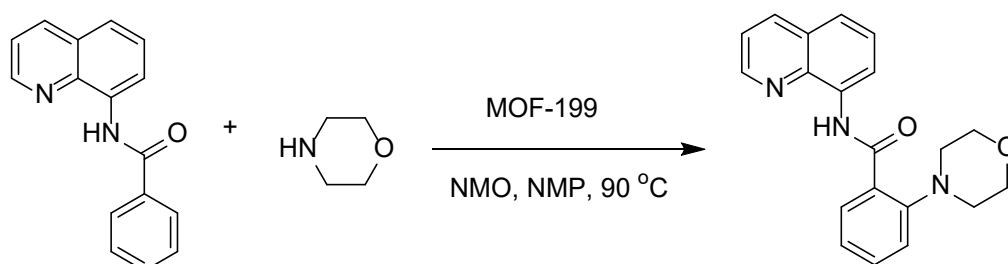
Among the various cross-coupling reactions and after the C-C cross-coupling, C-N is most probably the second most important coupling reaction, attracting widespread interest due to the application of the resulting products in the preparation of functional materials, sensors and as synthetic intermediates in the pharmaceutical industry.⁶⁵⁻⁶⁷ The reaction involves the use of oxygen or oxidizing agents to promote the coupling.

3.1 sp^2 C-H Activation

Direct amination of C-H bonds has been reported with homogeneous catalysts using palladium, iridium, and ruthenium complexes with appropriate ligands.^{68, 69} In one of these examples, the coupling between N-benzoyl-8-amino-quinoline and morpholine was effectively promoted by MOF-199 in 99 % yield using 20% AgOAc with N-methylmorpholine oxide as oxidant in N-methyl pyrrolidine as solvent at 90 °C (Scheme 17).⁴¹ The structure of MOF-199 (identical to HKUST-1) is constituted between Cu²⁺ clusters and BTC as linkers resulting in the formation of Cu₃(BTC)₂ possessing surface area around 1500 m²g⁻¹. Interestingly, other Cu-based MOFs, like Cu(BDC), Cu₂(BDC)(DABCO), Cu₂(BPDC)(BPY) and Cu₂(PDA)(BPY) (PDA: 1,3-phenylenediacetic acid) also afford the same coupling product in more than 90 % yield under identical conditions. In contrast, Ni₃(BTC)₂ and Co-MOF-74 (prepared by the reaction of cobalt nitrate hexahydrate with 2,5-dihydroxy benzenedicarboxylic acid) afforded 6 and 2 % yields under similar reaction conditions. The current catalytic data point to the superior activity of Cu-based MOFs in the presence of oxidant in polar solvent medium. The most probable reason of the Cu²⁺ MOFs superiority as catalyst to promote this C-N coupling is their ability to coordinate with the reagents, activating them in this way.

An analogous coupling in homogeneous phase using Cu(NO₃)₂ and CuCl₂ afforded, under identical conditions, 86 and 79 % yield, respectively. Comparing of the catalytic data between homogenous and heterogeneous catalysts, MOFs present many potential advantages, like tunability of composition and structure that could result in higher activity and reusability. Leaching experiments indicated that the activity of MOF-199 is due to the sites present in the solid. The catalyst was reused for five cycles without considerable decrease in its activity. Furthermore, powder XRD pattern of the five-times reused sample showed negligible changes in its crystallinity compared to that of the fresh material. Regarding the scope of the catalyst, a

large number of substituted benzoic acid derivatives were conveniently coupled with primary and secondary amine using morpholine oxide as oxidizing agent in moderate to high yields.



Scheme 17. C-N coupling between N-benzoyl-8-aminoquinoline and morpholine using MOF-199 as catalyst through oxidative C-H activation in NMP as solvent.

Quinoxalinone derivatives are synthetic intermediate for the preparation of important drug molecules with application in the formulation of pharmaceutical and agricultural products.⁷⁰⁻⁷² The structure of Cu-CPO-27 was reported by series of researchers and corresponds to a honeycomb-like MOF based on the coordination between Cu(II) ions with 2,5-dihydroxyterephthalic acid.^{73, 74} In this context, recently, a Cu-based MOF, Cu-CPO-27 (Figure 11) was reported as a solid heterogeneous catalyst promoting the coupling between quinoxalin-2(1H)-one with morpholine to give 3-morpholinoquinoxalin-2(1H)-one with 84 % yield using DMA as solvent at 80 °C under aerobic conditions (Scheme 18).⁴² Furthermore, the activity of Cu-CPO-27 was compared with that of a series of MOFs under identical experimental conditions. For instance, Fe-MOF-235 and Ni₂(BDC)₂(DABCO) showed no activity for the direct C-H amination to give 3-morpholinoquinoxalin-2(1H)-one. Also, Co-ZIF-67 as catalyst afforded an insatisfactorily low 17 % yield. In contrast, Cu MOFs displayed better performance than Fe-, Ni-, and Co-based MOFs. The use of Cu₃(BTC)₂ as solid catalyst afforded 39 % yield of the desired product under identical conditions, while the yield was increased to 47 % with Cu(BDC) as solid catalyst. Further, Cu₂(BDC)₂(DABCO) exhibited 63 % yield under similar conditions. Comparing these catalytic data, Cu-CPO-27 exhibits much

superior activity than any other tested Cu-MOF to activate C-H bond leading to 3-morpholinoquinoxalin-2(1H)-one. Interestingly, the optimized experimental conditions employing Cu-CPO-27 were also applied to the synthesis of a series of 3-aminoquinoxalin-2(1H)-ones reaching moderate to high yields of the coupling product. Leaching experiments confirmed that the reaction is successful only in the presence of Cu-CPO-27. Reusability tests indicated that Cu-CPO-27 can be recycled five times with no deterioration in its activity. The reused Cu-CPO-27 showed in FT-IR spectroscopy comparable vibration bands to that of the fresh sample while powder XRD analysis disclosed the unchanged crystallinity of the framework in the reused material compared to fresh one. A possible mechanism (Figure 12) has been proposed for this transformation promoted by Cu-CPO-27, but, however, further studies are required to validate these assumptions.

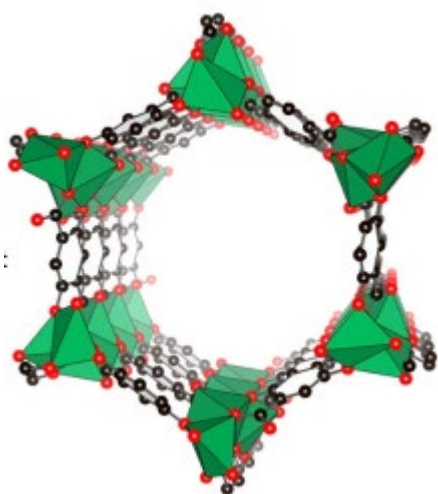
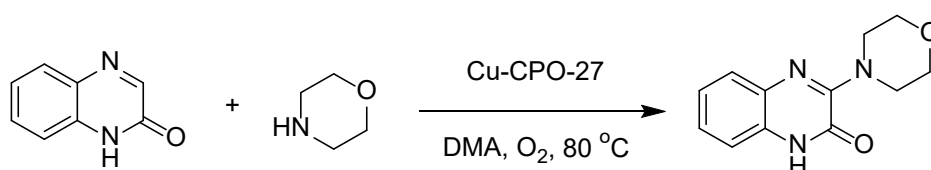


Figure 11. The structure of Cu-CPO-27. Reprinted with permission from ref.42 Copyright 2017 Elsevier.



Scheme 18. C-N bond formation between quinoxalin-2(1H)-one with morpholine using Cu-CPO-27 as solid catalyst.

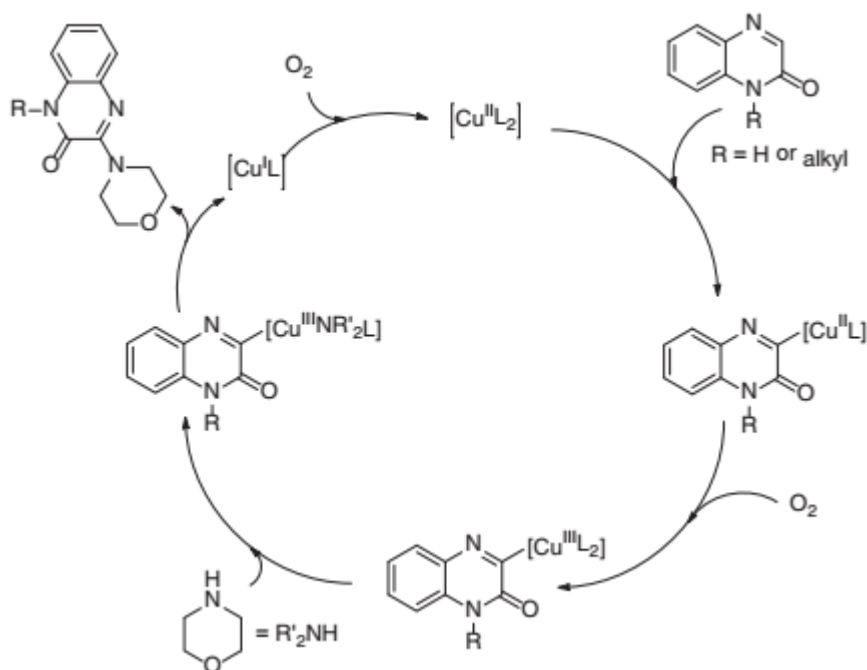


Figure 12. A possible mechanism for the C-N bond formation by Cu-CPO-27. Reprinted with permission from ref.42 Copyright 2017 Elsevier.

A highly porous MOF, 537-MOF with molecular formula $\{[Cu_2(TPPB)_2](DMF)_6\}$ was synthesised. Single-crystal X-ray diffraction analysis indicated that 537-MOF crystallizes in the triclinic space group. The Cu1 and Cu2 atoms in its structure are bridged by four carboxylate groups from TPPB²⁻ ligand. Each TPPB²⁻ ligand (see Figure 13) binding to three 6-connected paddlewheel dimers leads to the assembly of a (3,6)-connected rtl network with pores of 0.51 nm as shown in Figure 13. The catalytic activity of 537-MOF was tested in the synthesis of benzimidazoles through the activation of C-H bond under air atmosphere.⁴³ Among the various conditions tested for the conversion of amidine to 2-phenylbenzimidazole (Scheme 19), the yield of the final product was 96 % in a mixed solvent of DMSO/DMF and benzoic acid as additive. It was believed that the use of benzoic acid suppressed the

decomposition of products under this condition. Furthermore, functionalized amidines possessing electron-withdrawing, and donating substituents were converted under optimal reaction conditions into their corresponding benzimidazoles in moderate to high yields. The catalyst was recycled for three runs with no drop in the yield. In addition, powder XRD of the recovered catalyst showed identical crystalline pattern compared to that of the fresh solid sample suggesting the stability during the course of the reaction.

Figure 14 shows two possible paths for the conversion of aldimines to 2-phenylbenzimidazole. In the first path, 537-MOF is coordinated to amidines which is followed by electrophilic addition to copper center to N-phenyl ring to provide the intermediate B. Later, B undergoes reductive elimination of the metal centre followed by rearomatization to give final product D. In the second path, the amidine reacts with 537-MOF to generate copper nitrene intermediate C. Later, this intermediate undergoes series of concerted steps like insertion of the nitrogen into a C–H bond of amidine, electrocyclic ring closure and subsequent [1,3]-shift of a hydrogen to afford the final product D.

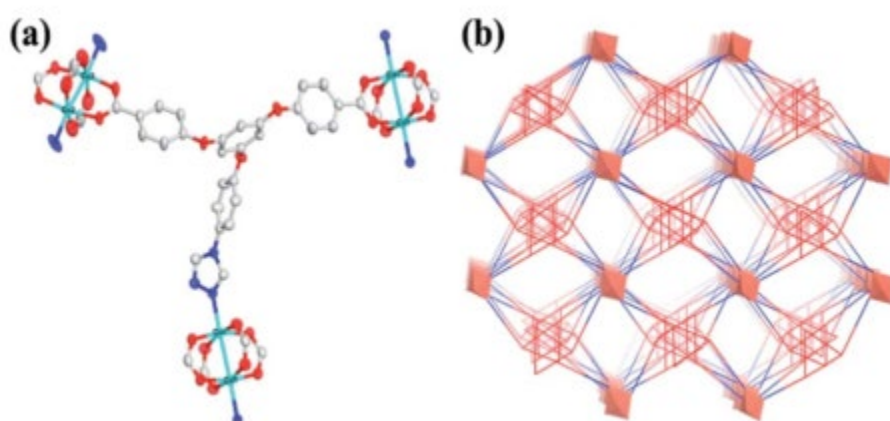
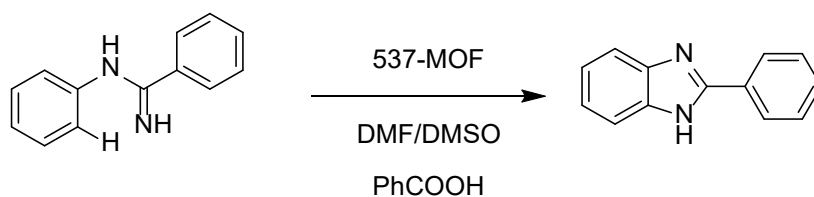


Figure 13. (a) Illustration of the coordination mode of TPPB²⁻ ligand and (b) view of (3,6)-connected rtl topology of 537-MOF. Reprinted with permission from ref.43 Copyright 2017 Royal Society of Chemistry.



Scheme 19. Conversion of amidine to 2-phenylbenzimidazole using 537-MOF in DMF/DMSO with benzoic acid as additive.

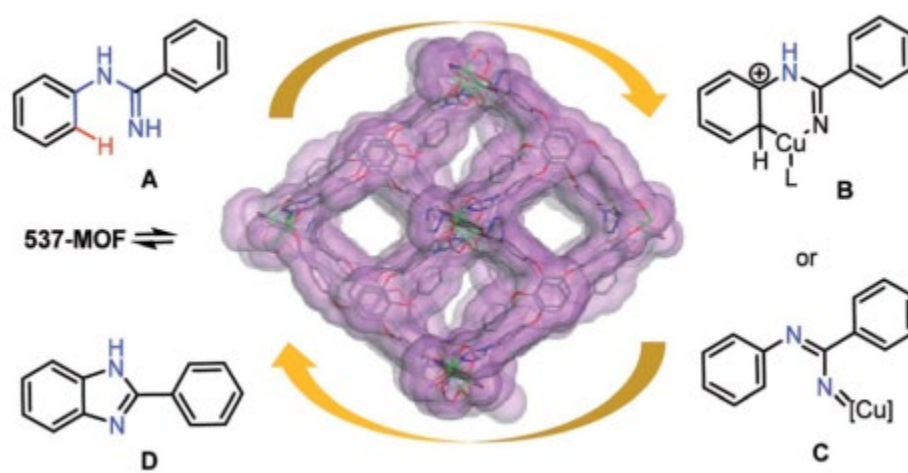


Figure 14. A proposed mechanism for the C-H functionalization of amidine by 537-MOF. Reprinted with permission from ref.43 Copyright 2017 Royal Society of Chemistry.

3.2 sp^3 C-H Activation

Among the most extensively used MOFs as catalysts in organic transformations, copper-based MOFs with coordinatively unsaturated metal sites^{58, 75, 76} exhibited a wide range of catalytic activity. Most of the reported Cu-based MOFs have been synthesized using a copper salt and aromatic carboxylates as linkers resulting in Cu-oxo cluster with four coordination positions either in tetrahedral, distorted tetrahedral, or square planar geometry.⁷⁷ Generally, these Cu MOFs exhibit low chemical stability under vigorous reaction conditions or in the presence of the reagents and solvents that can act as Cu ligands or reducing agents.^{78,}

⁷⁹ In this context, recently, a copper-based MOF was prepared (VNU-18) starting from copper

nitrate and using a 3,5-pyridinedicarboxylic acid (PDC) as linker. The structure of VNU-18 is presented in Figure 15. The activity of VNU-18 with regard to their catalytic activity in the oxidative cross coupling between ethyl phenyl ketone and morpholine was compared with those of a series of other Cu-based MOFs possessing tetrahedral sites.⁴⁴ Activity data revealed that VNU-18 exhibits 84 % yield with around 5 ppm of Cu, while other MOFs like $\text{Cu}_3(\text{BTC})_2$, $\text{Cu}(\text{BDC})$, $\text{Cu}_2(\text{BDC})_2(\text{BPY})$, $\text{Cu}_2(\text{BDC})_2(\text{DABCO})$ and $\text{Cu}_2(\text{BPDC})(\text{BPY})$ afforded the expected product with lower yields in the range of 35-65 %. Moreover, except VNU-18, the other Cu MOFs exhibited considerable Cu leaching (56 to 105 ppm) under identical conditions. These catalytic data clearly prove the superiority of VNU-18 providing high efficiency in this oxidative C-N coupling reaction as heterogeneous catalyst. In contrast, other Cu-MOFs possessing four coordination sites were not sufficiently stable under the reaction conditions leading to a considerable percentage of free Cu species in the solution. Interestingly, VNU-18 was used as catalyst to prepare a series of molecules of interest as therapeutical drugs. The synthesis starts from commercial substrates to produce racemic mixtures of clopidogrel (Plavix), amfepramone, α -pyrrolidinovalerophenone and other dopamine transporters in reasonable yields (Scheme 20).

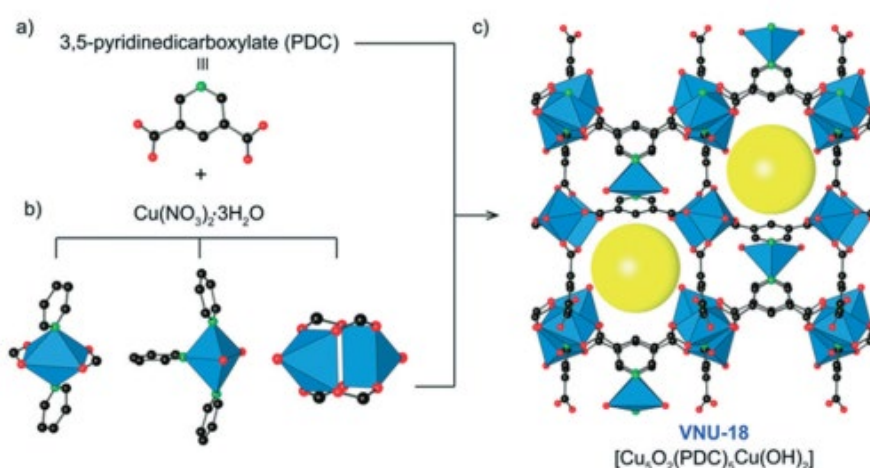
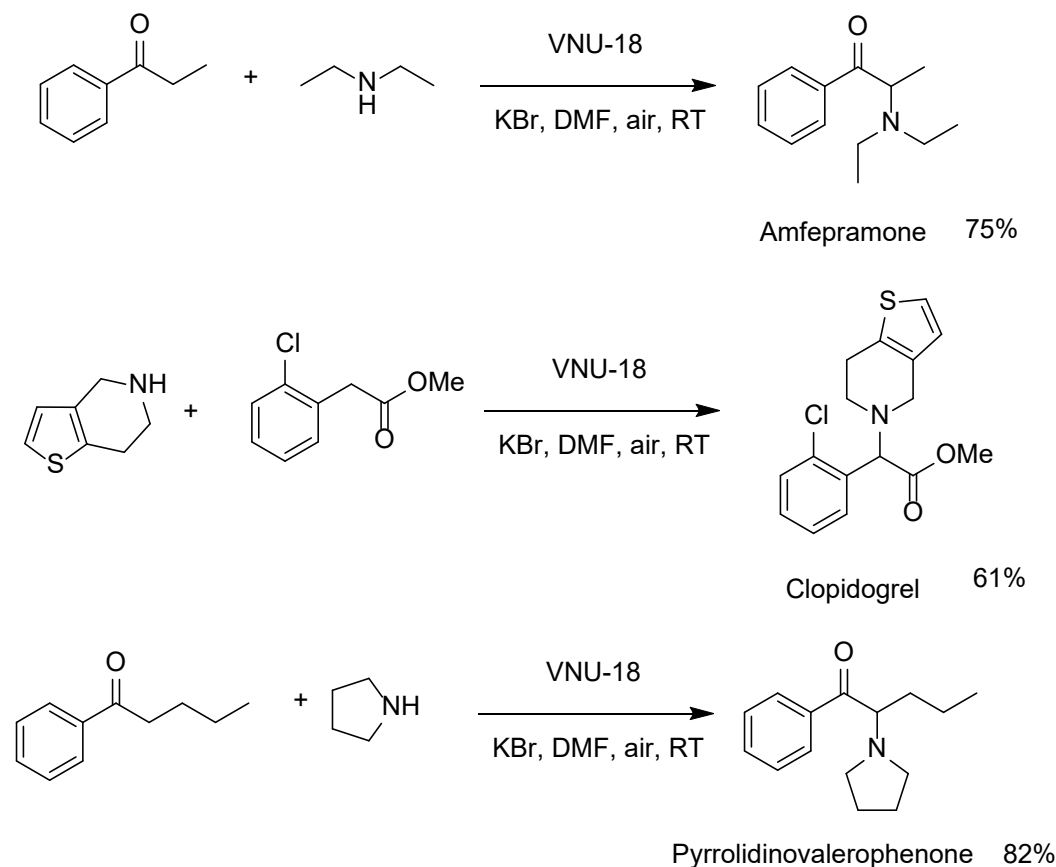


Figure 15. Structure of PDC (a), three kinds of Cu building blocks (b) and the formation of VNU-18 (c). The yellow balls display the pore size of 14 Å as calculated for VNU-18. Reprinted with permission from ref.44 Copyright 2017 Royal Society of Chemistry.



Scheme 20. Synthesis of medicinally important molecules using VNU-18 as a solid catalyst.

Recently, CPF-5 was synthesised⁸⁰ by the reaction between MnCl_2 , TZBA and ammonium formate resulting in the formation of a MOF with the molecular formula $\text{Mn}_{21}(\text{TZBA})_{12}(\text{HCO}_2)_{18}(\text{H}_2\text{O})_{12}$ containing unsaturated Mn^{II} sites. The crystal structure reveals that three framework tetrazolate rings bind one Mn^{II} center on each corner of the SBU to form an isolated tripodal Mn^{II} site with pores about 1.3 nm (Figure 16). The catalytic activity of CPF-5 (1 mol%) was examined in the intermolecular C-H amination between tetrahydrofuran and phenyl-N-tosylidiodane ($\text{PhI}=\text{NTs}$, Scheme 21) in acetonitrile at room temperature in 30 min.⁴⁵ Analysis of the reaction mixture by $^1\text{H-NMR}$ spectroscopy and GC-

MS indicated the expected product formation of N-(tetrahydro-2-furanyl)-4-toluenesulfonamide at 85 % yield. The structural integrity of CPF-5 after catalysis was also confirmed by powder XRD and gas sorption measurements. Hot filtration tests proved the heterogeneity of the reaction. ICP-MS analysis indicated Mn leaching in a concentration around 5 ppb. On the other hand, homogeneous Mn^{II} complexes (5 mol %) provided lesser yields of the corresponding amination products with values ranging between 32-38 % after 1 h under identical conditions. A series of Mn salts [(Mn(acac)₃, MnCO₃, Mn(OAc)₂)] and a selection of MOFs [UiO-66(Zr), ZIF-8(Zn), ZIF-67(Co)] were also tested for this reaction under similar experimental conditions, but no product was observed. The substrate scope using CPF-5 was wide as shown in Scheme 22. Interestingly, a large-scale reaction between PhI=NTs and dihydroisobenzofuran was performed in the presence of 1 mg of CPF-5 catalyst under identical conditions. This reaction afforded 89 % yield after 2.5 h with a turnover number (TON) of about 120000 and turnover frequency (TOF) value of around 48000 h⁻¹ (Scheme 23). This productivity experiment with a large excess of substrate clearly demonstrated that CPF-5 is an extremely efficient catalyst compared to the homogeneous and other heterogeneous MOF counterparts.

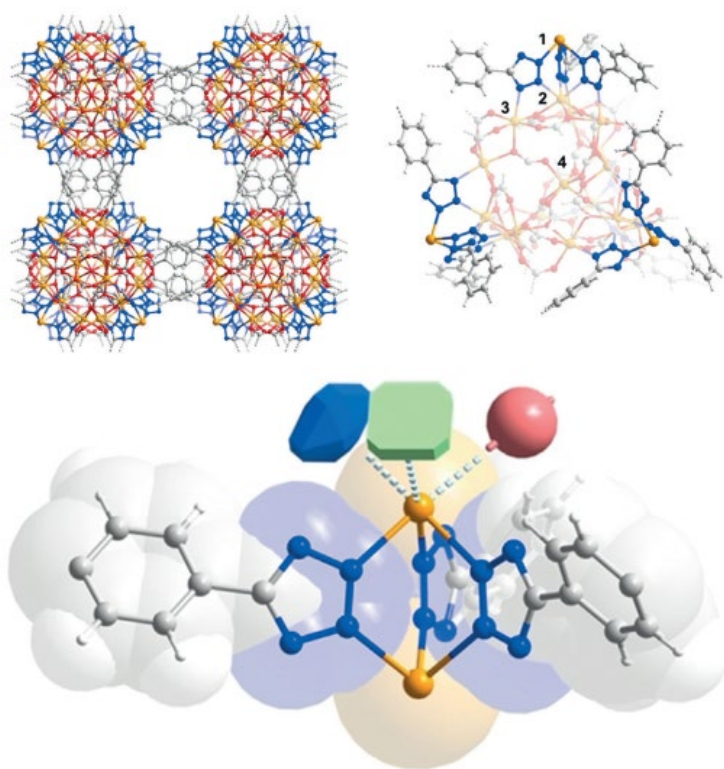
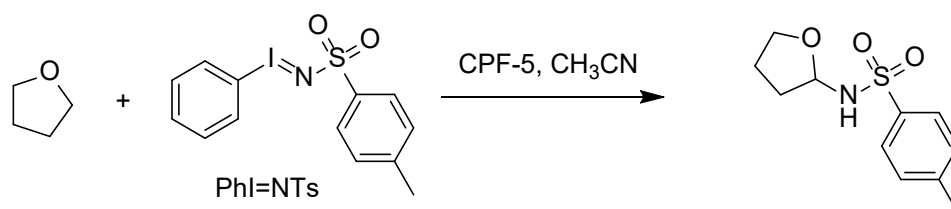
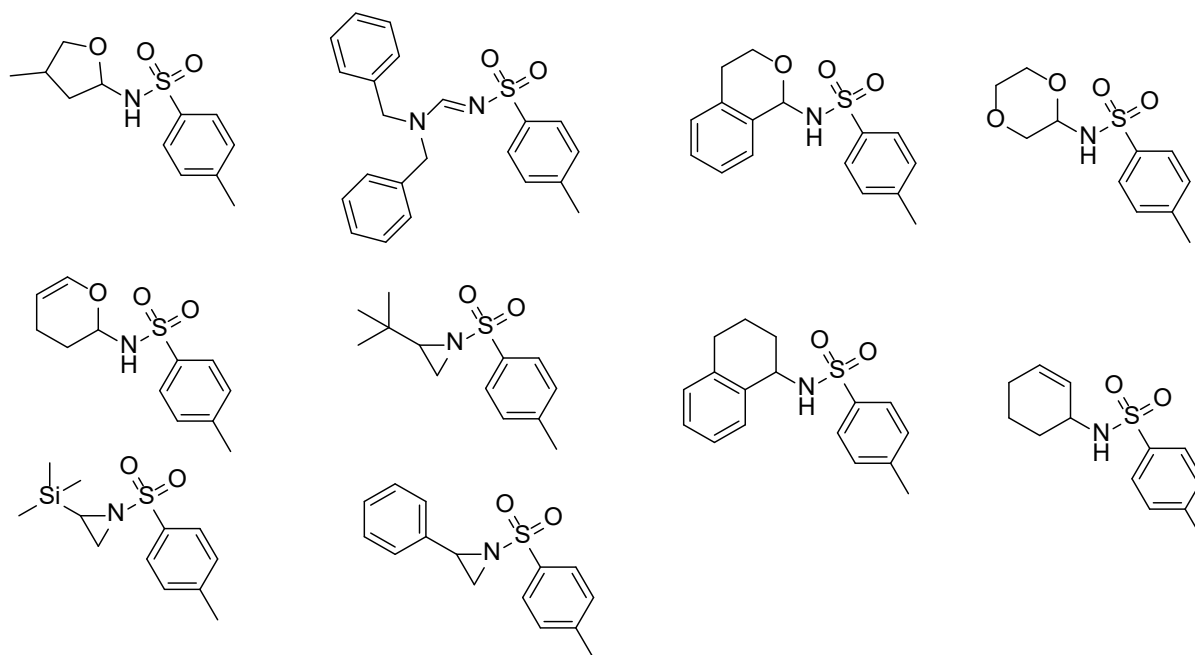


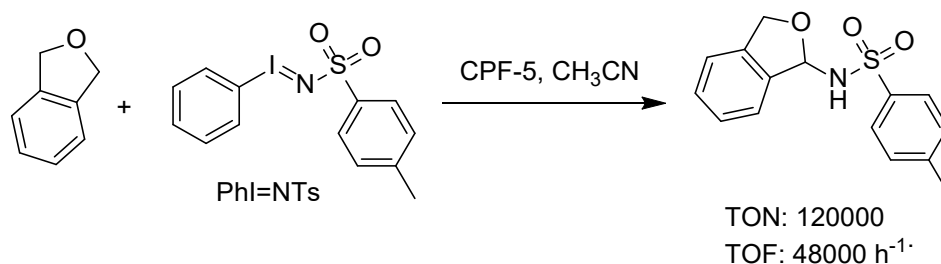
Figure 16. Structure of CPF-5 showing complex SBUs and large 13.6 Å pores (top left). The SBUs contain four crystallographically independent Mn^{II} ions (top right, labelled as Mn1-4), with the tripodal active (Mn1) active site highlighted in darker color. The facially coordinated Mn^{II} in CPF-5 possesses open coordination sites for substrate binding (bottom, depicted as different colored shapes). Mn orange, C gray, H white, N blue, O red. Reprinted with permission from ref.45 Copyright 2018 Wiley.



Scheme 21. CPF-5 catalyzed amination of tetrahydrofuran at room temperature.



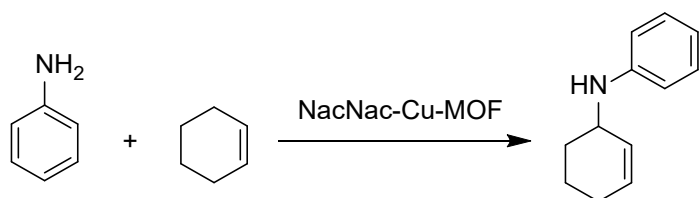
Scheme 22. Scope of the toluenesulfonamide coupling catalyzed by CPF-5.



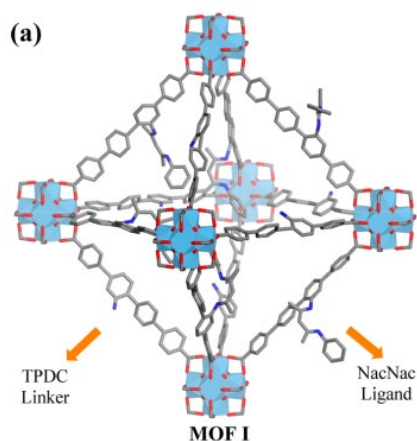
Scheme 23. Amination of dihydroisobenzofuran with PhI=NTs using CPF-5 as catalyst.

β -Diketiminato ligands known as NacNac are a useful class of bidentate ligands with the ability to form coordination complexes with a wide range of metals.⁸¹ In this aspect, a post-synthetic installation of the β -diketiminato functionality was performed in a UiO-based MOF (Figure 17).⁴⁶ Metalation of the NacNac-MOF (**I**) with copper metal salt resulted in the formation of the expected MOF-supported NacNac-Cu. The NacNac-Cu-MOF catalyst was highly active in catalyzing the intermolecular C-H amination of cyclohexene (Scheme 24) with aniline to provide secondary amine in excellent selectivity.⁴⁶ The use of 2 mol % NacNac-Cu-MOF for the reaction of aniline and cyclohexene resulted in 22% yield of N-(cyclohex-2-en-

1-yl)aniline in benzene. The yield of the desired product was enhanced to 67% in neat cyclohexene conditions. Further, increasing the loading of NacNac-Cu-MOF to 3 mol % afforded 90 % yield under identical conditions. Interestingly, NacNac-Fe-MOF did not show any activity for this reaction, thus suggesting the dependence of the metal attached to NacNac linker. On other hand, control experiments using homogeneous and heterogeneous NacNac-Cu-MOF catalysts for the reaction of 2,4,6-trimethylaniline and cyclohexene exhibited size-selective intermolecular amination reaction. The activity of NacNac-Cu-MOF (3 mol %) was retained for five cycles with no decrease in product yield. Powder XRD studies revealed that the MOF crystallinity is retained during the course of reaction.



Scheme 24. NacNac-Cu-MOF catalyzed C-H amination of cyclohexene.



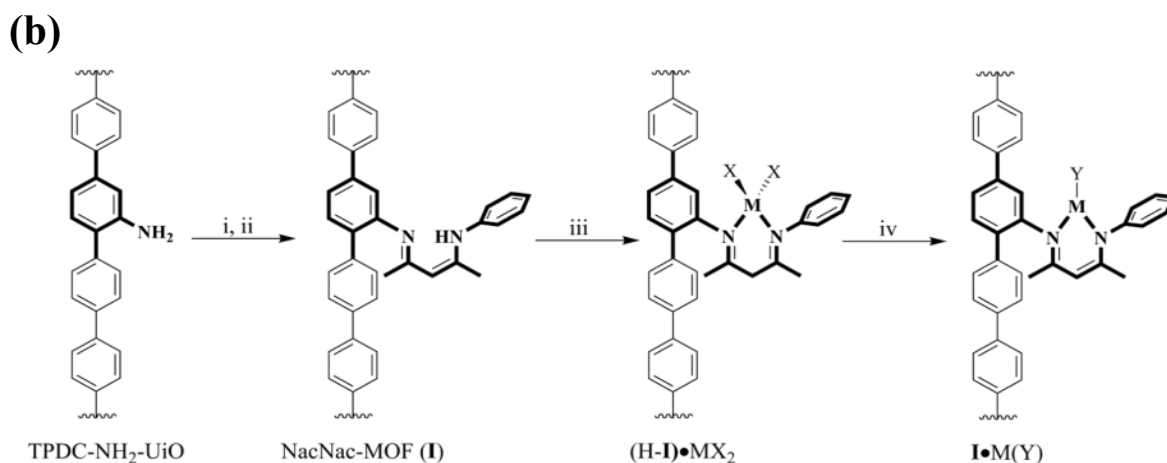
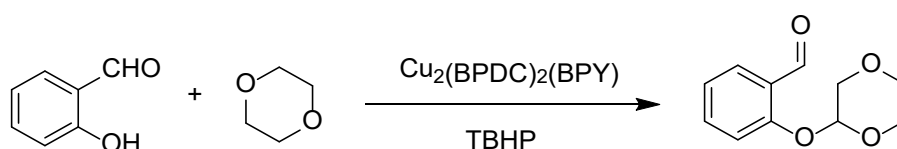


Figure 17. (a) Structural model showing the octahedral cage of NacNac-functionalized MOF; (b) Synthesis route showing NacNac installation and metalation: (i) Et₃OBF₄ (1.1 equiv of w.r.t. amino ligand), 4-N-phenylamino-3-penten-2-one (1.1 equiv of w.r.t. amino ligand), DCM. (ii) KOTu (0.7 equiv of w.r.t. amino ligand). (iii) Cu(MeCN)₄PF₆ (0.6 equiv of w.r.t. amino ligand) in THF. (iv) KOTu (1 equiv of w.r.t. Cu). Reprinted with permission from ref. 46 Copyright 2016 American Chemical Society.

4. C-O Bond Formation

Cross-coupling reactions leading to the formation of carbon–carbon and carbon–heteroatom bonds are often catalyzed by transition metals and considered as a versatile method in organic chemistry.⁸²⁻⁸⁵ After C-C and C-N bond formations, other C-heteroatom bonds are also important and can be promoted using MOFs as heterogeneous catalysts. Regarding C-O bond formation also the presence of oxidants is needed. Thus, the reaction between 2-hydroxybenzaldehyde and 1,4-dioxane has been reported to be efficiently catalyzed by Cu₂(BPDC)₂(BPY) MOF, achieving 100 % conversion at 100 °C using TBHP as oxidant through the C-H activation of 1,4-dioxane. The C-O bond formation between 2-hydroxybenzaldehyde and 1,4-dioxane is shown in Scheme 25.⁴⁷ Furthermore, the activity of Cu₂(BPDC)₂(BPY) was superior than that of Cu₃(BTC)₂, Cu(BDC), and Cu(BPDC) MOFs

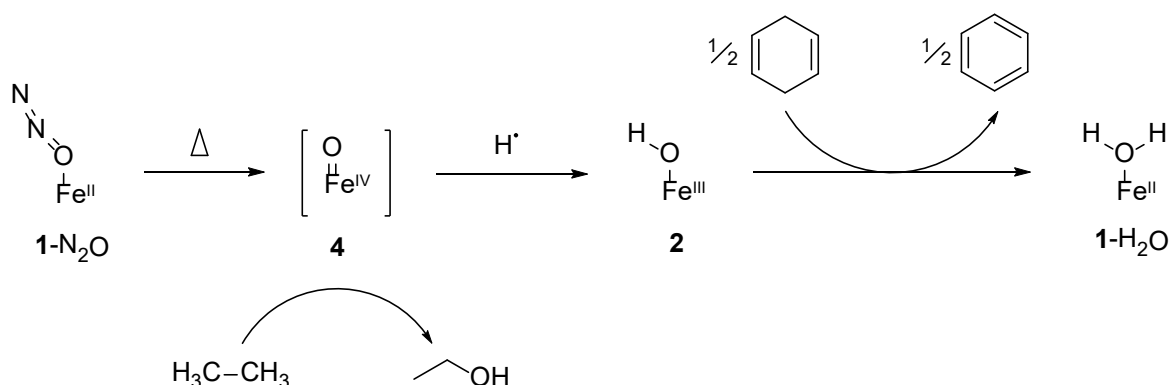
under identical conditions. The activity of $\text{Cu}_2(\text{BPDC})_2(\text{BPY})$ was retained without significant decay for eight runs. Powder XRD of the reused $\text{Cu}_2(\text{BPDC})_2(\text{BPY})$ showed identical pattern as the fresh solid, while the FT-IR spectra of fresh and reused samples were similar. The process was heterogeneous in nature. Interestingly, $\text{Cu}_2(\text{BPDC})_2(\text{BPY})$ was able to promote this coupling reaction with complete conversion in 100 min, while $\text{Cu}(\text{OAc})_2$ required 120 min to reach 87 % conversion under identical conditions. These results indicate the superiority of MOF catalyst in terms of activity. In addition, $\text{Cu}_2(\text{BPDC})_2(\text{BPY})$ can be readily reused without loss in activity.



Scheme 25. The dehydrogenative cross-coupling between 2-hydroxybenzaldehyde and 1,4-dioxane promoted by TBHP using $\text{Cu}_2(\text{BPDC})_2(\text{BPY})$ as catalyst.

Recently, the iron-based MOF $\text{Fe}_2(\text{dobdc})$ (dobdc^{4-} : 2,5-dioxido-1,4-benzenedicarboxylate) and its mixed-metal analogue $\text{Fe}_{0.1}\text{Mg}_{1.9}(\text{dobdc})$ has been reported as heterogeneous solid catalysts to effect the activation of C-H bonds in ethane using nitrous oxide as the terminal oxidant (Scheme 26).⁴⁸ The flow of a mixture of N_2O : ethane: Ar over the framework of $\text{Fe}_2(\text{dobdc})$ resulted in the formation of ethanol, acetaldehyde, diethyl ether and other oligomers at 75 °C. It was believed that the formation of complex mixture of oxygenated products is due to the close proximity of reactive iron centres with ethane. In contrast, the interaction of $\text{Fe}_{0.1}\text{Mg}_{1.9}(\text{dobdc})$ with N_2O and ethane under similar conditions showed the exclusive formation of ethanol and acetaldehyde in a 10:1 ratio with a yield of 60 %. In addition, detailed reactivity studies, characterization of decay products and theoretical calculations indicated that $\text{Fe}_2(\text{dobdc})$ and $\text{Fe}_{0.1}\text{Mg}_{1.9}(\text{dobdc})$ are very likely capable of forming an active oxidant of iron(IV)-oxo species having an unusual $S=2$ spin state. In another report,

a detailed mechanistic study has proved that $\text{Fe}_{0.1}\text{Mg}_{1.9}(\text{dobdc})$ activates the strong C–H bonds in ethane through the formation of iron(IV)-oxo sites.⁸⁶

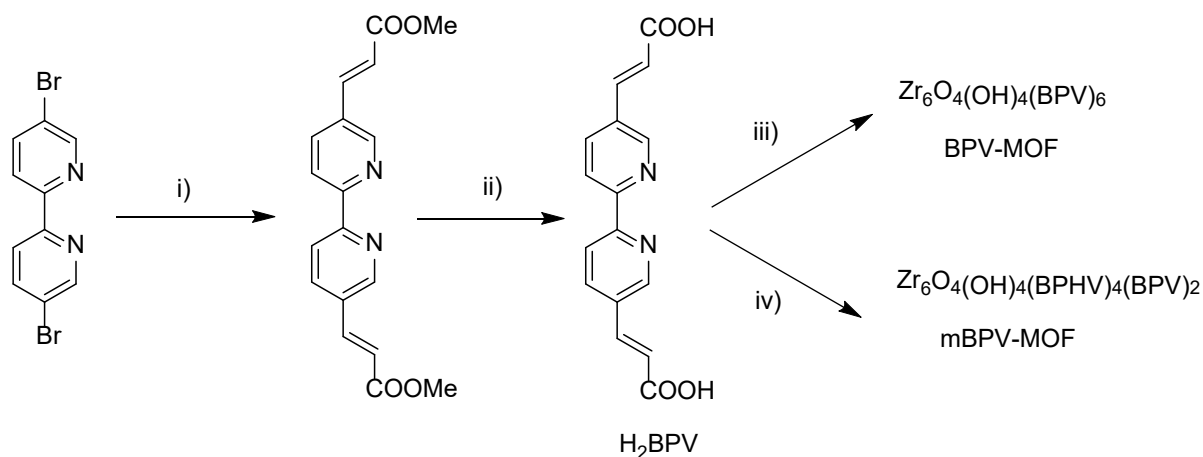


Scheme 26. N_2O activation and reactivity of $\text{Fe}_2(\text{dobdc})$ in the oxidation of ethane and 1,4-cyclohexadiene. Heating of N_2O -bound $\text{Fe}_2(\text{dobdc})$ ($1\text{-N}_2\text{O}$) to $60\text{ }^\circ\text{C}$ results in the formation of a transient high-spin $\text{Fe}^{\text{IV}}\text{-oxo}$ species (4), which can react with the strong C–H bonds of ethane. In the absence of a hydrocarbon substrate, the $\text{Fe}^{\text{IV}}\text{-oxo}$ quickly decays via hydrogen-atom abstraction into an $\text{Fe}^{\text{III}}\text{-hydroxide}$ (2), which is isolable and well characterized. This hydroxide species can react with weak C–H bonds, such as those in 1,4-cyclohexadiene, to form benzene and H_2O -bound $\text{Fe}_2(\text{dobdc})$ ($1\text{-H}_2\text{O}$). Adapted from ref. 48

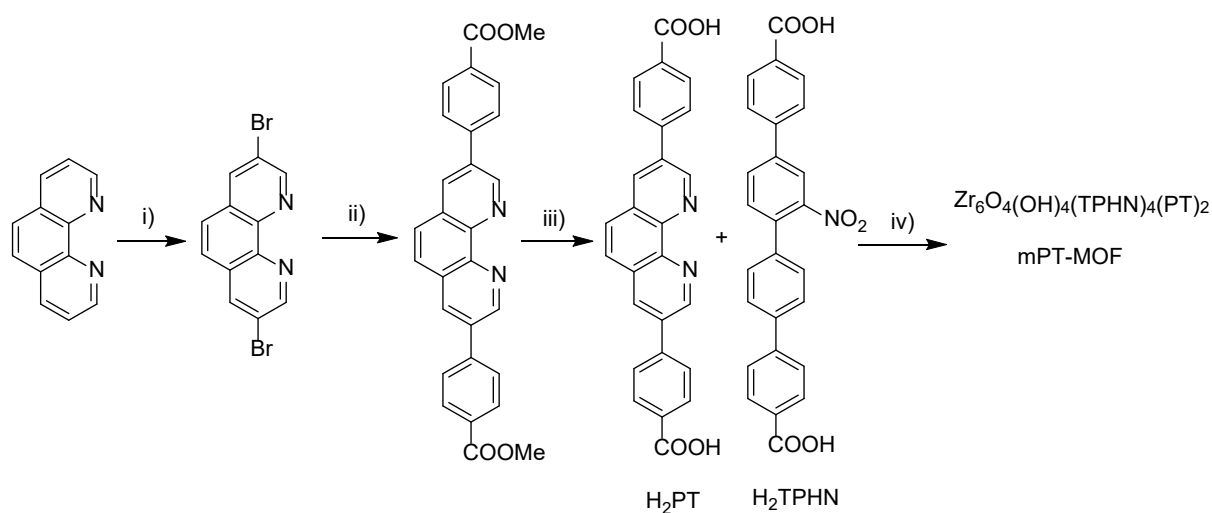
5. C-B Bond Formation

A series of robust and porous MOFs with UiO-67 topology using bipyridyl- (BP) and phenanthryl- (PT) based ligands (BPV-MOF, mBPV-MOF, and mPT-MOF; “m” stands for mixed) were synthesised as illustrated in Schemes 27 and 28. Subsequent post-synthetic metalation allowed to form an Ir complex attached to the MOF ligands resulting in BPV-MOF-Ir, mBPV-MOF-Ir, and mPT-MOF-Ir.⁴⁹ A mixed linker strategy was used for the preparation of these MOFs combining in the synthesis of functionalized (4,4'-biphenylenedicarboxylic acid) and unfunctionalized linkers to obtain mixed-linker MOFs possessing much larger open channels and pores and a controlled density of active sites which can facilitate the diffusion of

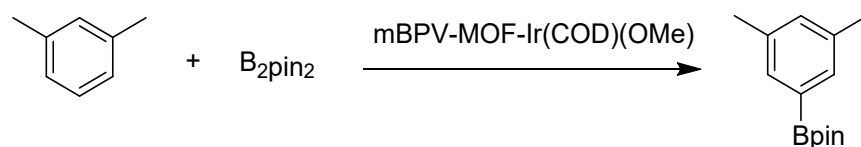
reactants and products within the porous MOFs respect to the analogues material prepared exclusively with the BP or PT ligands. The activity of these Ir-containing mixed ligand MOFs was investigated in the C-H borylation of arenes with B_2pin_2 . BPV-MOF was obtained from only bipyridyl-functionalized dicarboxylate linker, whereas both mBPV- and mPT-MOFs were constructed using a mixture of bipyridyl- or phenanthryl functionalized and unfunctionalized 4,4'-biphenylene dicarboxylate linkers (Schemes 27 and 28). Interestingly, mBPV-MOF-Ir and mPT-MOF-Ir catalysts exhibited significantly higher activity than their corresponding homogeneous analogues in the borylation of m-xylene with B_2pin_2 (Scheme 29) at 115 °C under nitrogen atmosphere. The kinetic data revealed that mBPV-MOF-Ir was 95 times more active than $[bpy(CH=CHCO_2Me)_2]Ir(COD)-(OMe)$ as soluble analogue with a TON value of 17000. In contrast, $[bpy(CH=CHCO_2Me)_2]-Ir(COD)(OMe)$ gave only 9 % conversion under identical conditions. On other hand, the activity of mPT-MOF-Ir was twice than that of its homogeneous counterpart. The mBPV-MOF-Ir catalyst was recycled more than 15 times without significant decay in its activity in the borylation of indole with B_2pin_2 at 115 °C. Further, powder XRD did not show any loss in its crystallinity after recycling. The catalysis using mBPVMOF-Ir was found to be heterogeneous in nature and leaching of Ir and Zr during the course of the reaction could not be observed. In another experiment, mPT-MOF-Ir was recycled 15 times in the borylation of m-xylene. However, although powder XRD of recovered mPT-MOF-Ir after 17th cycles showed that the crystal structure of MOF is still preserved, the activity loss was interpreted as being derived from the decomposition of Ir complex anchored in mPT-MOF-Ir upon many consecutive runs.



Scheme 27. Synthesis of BPV-MOF and mBPV-MOF. Reaction conditions: (i) methyl acrylate, Pd(OAc)₂, P(o-tol)₃, NEt₃, DMF, 120 °C, 2 d; (ii) NaOH, EtOH, H₂O, reflux; (iii) ZrCl₄, DMF, TFA, 100 °C, 5 d; (iv) H₂BPHV, ZrCl₄, DMF, TFA, 100 °C, 5 d.



Scheme 28. Synthesis of mPT-MOF. Reaction conditions: (i) Br₂, S₂Cl₂, pyridine, n-BuCl, reflux, 12 h; (ii) 4-methyl carboxyphenylboronic acid, Pd(PPh₃)₄, CsF, DME, 100 °C, 3 d; (iii) aq. NaOH, EtOH; (iv) ZrCl₄, DMF, TFA, 100 °C, 5 d.



Scheme 29. Borylation of m-xylene with B₂pin₂ using mBPV-MOF-Ir catalysts.

Organoboronic compounds have been conveniently prepared by C-H borylation with B_2pin_2 . Although sufficient methods have been developed for C-H borylation with arenes in last decades,⁸⁷⁻⁸⁹ no much attention has been paid to the benzylic C-H borylation. In this aspect, recently, a terpyridine-based metal-organic layer (TPY-MOL) was prepared. Metalation of TPY-MOL with $CoCl_2$ provided $CoCl_2.TPY-MOL$.⁵⁰ Figure 18 shows the structure of this $CoCl_2.TPY-MOL$. The activity of $CoCl_2.TPY-MOL$ was examined in the benzylic C-H borylation of methylarenes with B_2pin_2 (Scheme 30). Upon activation with $NaEt_3BH$, $CoCl_2.TPY-MOL$ (0.5 mol%) promoted m-xylene borylation with B_2pin_2 to achieve 42 % yield with a 4.2 : 1 selectivity favouring the benzylic position at 100 °C. Further, the yield of the borylated products was enhanced to 95 % with a higher selectivity for benzylic borylation (4.6 : 1) with 1 mol% catalyst. This borylation reaction failed if the activation of $CoCl_2.TPY-MOL$ is not performed with $NaEt_3BH$. The $CoCl_2.TPY-MOL$ was activated by $NaEt_3BH$ in THF to afford $CoH_2.TPY-MOL(II)$ intermediate, which quickly undergoes reductive elimination to provide H_2 as shown in Figure 19. On the other hand, a control experiment with TPY-MOF, whose structure is isostructural to BTB-MOF (BTB: 1,3,5-benzenetribenzoate) in which 2D layers connected in a staggered fashion resulting in 3D MOF⁹⁰ afforded no conversion under identical conditions. This lack of catalytic activity of the TPY-MOF may be due to the diffusion limitations experienced by the substrates to reach the active sites in a 3D material. In contrast, homogeneous $CoCl_2.TPY$ exhibited 2 % of the arene C-H borylation product. These catalytic data indicate that active site isolation in metal-organic layers not only enhances the TON more than 20 times compared to homogeneous catalyst, but also provides unusual borylation selectivity towards benzylic C-H bond. $CoCl_2.TPY-MOL$ efficiently converted in high yields a series of methylarenes to their respective borylated products under the optimized reaction conditions. The activity of $CoCl_2.TPY-MOL$ was maintained for at least ten cycles without any noticeable decay in activity in the C-H borylation of p-xylene. Powder XRD of the recovered

$\text{CoCl}_2 \cdot \text{TPY-MOL}$ remained identical to that of the fresh material. Available data support that the catalysis was a heterogeneous process and ICP-MS showed that the Co and Hf leaching to the liquid reaction mixture was 0.092 and 0.037 %, respectively.

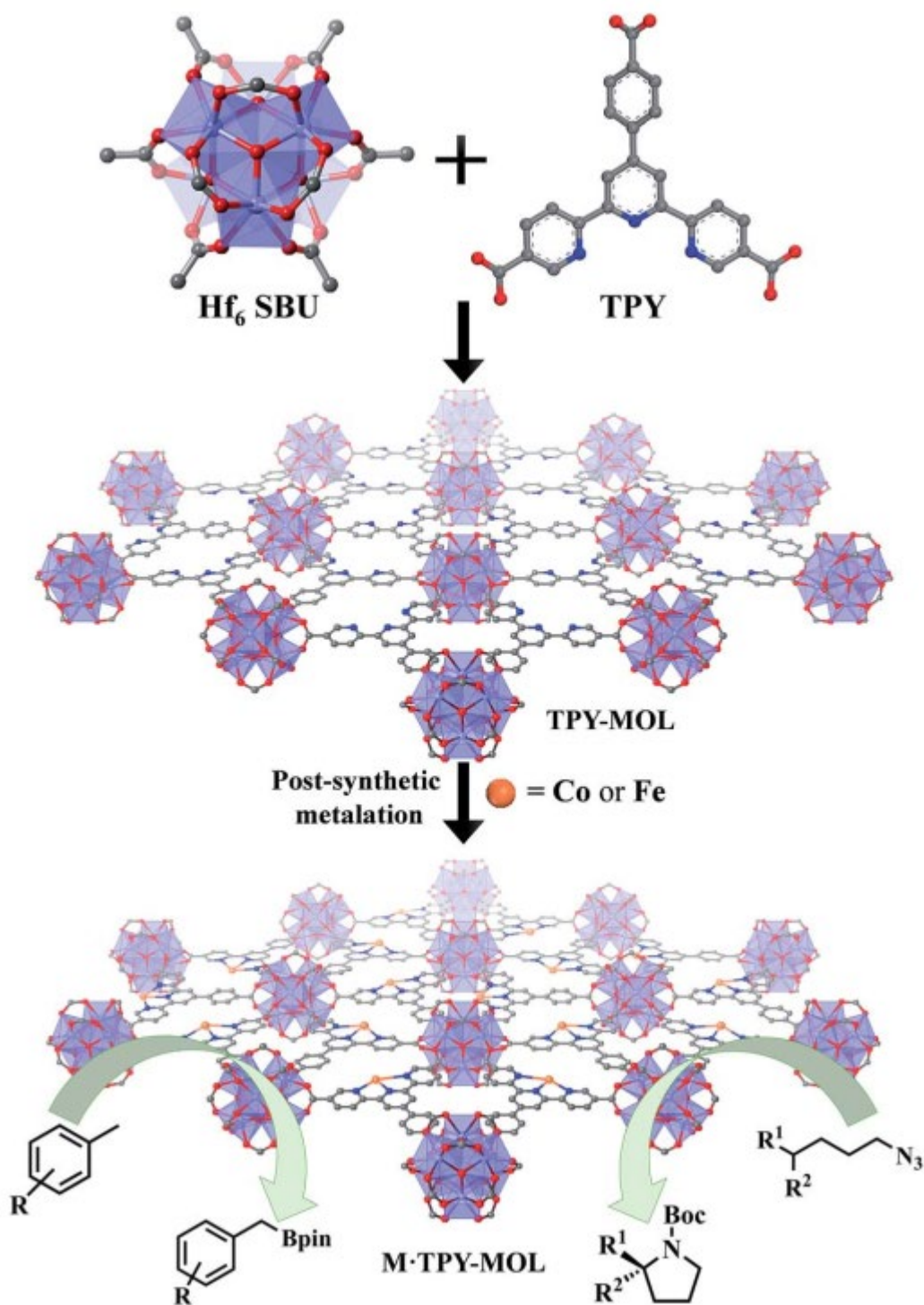


Figure 18. Structure of Hf_6 secondary building units and TPY forming TPY-MOL followed by metalation to obtain M.TPY-MOLs ($\text{M}=\text{Co}^{2+}$ or Fe^{2+}). Reprinted with permission from ref.50 Copyright 2018 Royal Society of Chemistry.

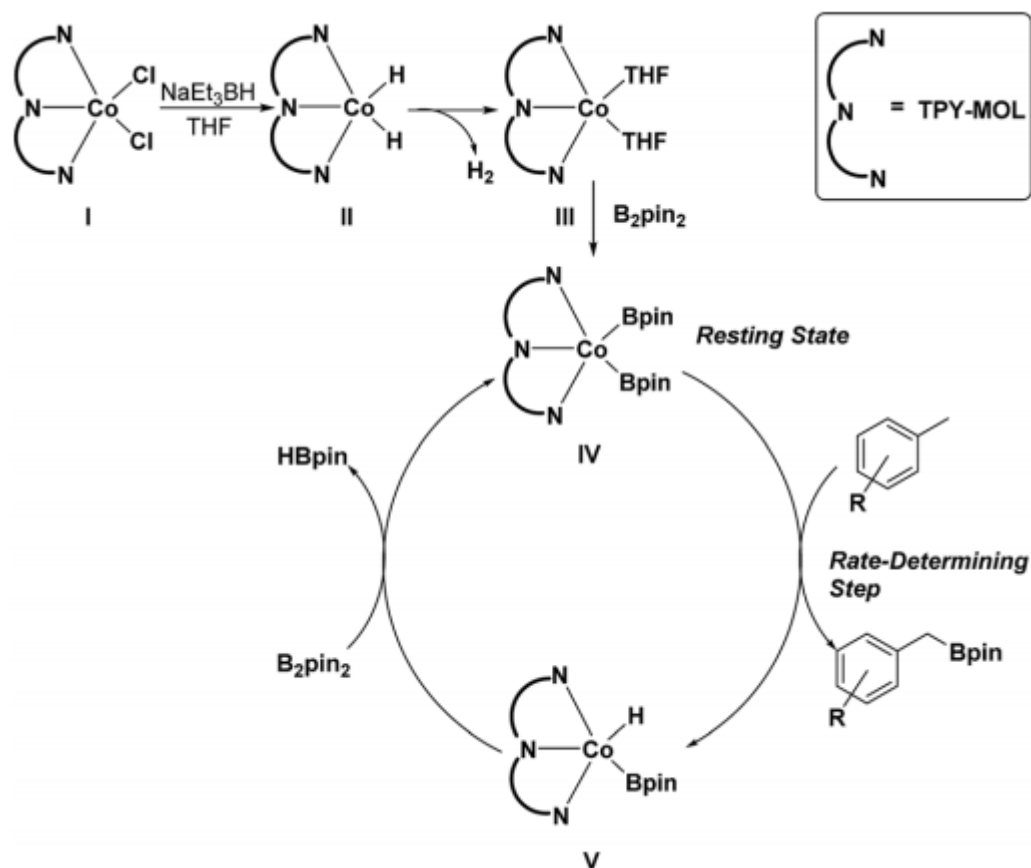
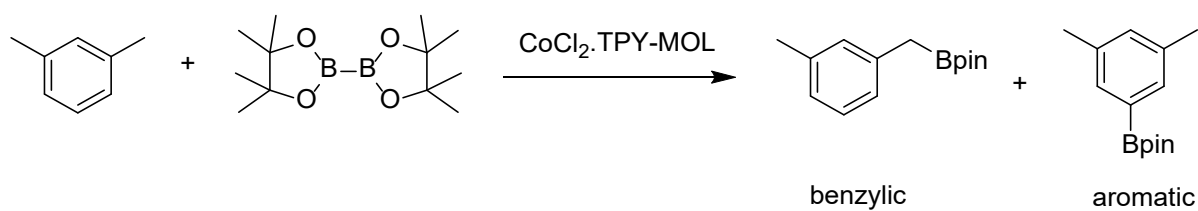


Figure 19. Proposed mechanism for the $\text{CoCl}_2 \cdot \text{TPY-MOL}$ catalyzed C-H borylation of arenes with B_2pin_2 . Reprinted with permission from ref.50 Copyright 2018 Royal Society of Chemistry.



Scheme 30. C-H borylation of m-xylene using B_2pin_2 by $CoCl_2.TPY-MOL$ catalyst.

6. C-X Bond Formation

MIL-101(Cr)- NH_2 was analogous structure to MIL-101(Cr) which has the pore size distribution of 1.54 and 1.99 nm, which are smaller than with MIL-101(Cr) due to the presence of amino groups occupying into the pores. MIL-88B- $NH_2(Fe)$ was synthesised by the reaction between Fe^{3+} with 2-aminoterephthalic acid as a linker. Halogenation of organic compounds is a key reaction in many organic syntheses. Hence, a convenient and selective method has been reported for heterogeneous C-H halogenation with Pd NPs immobilized over MIL-88B- $NH_2(Fe)$ [Pd@MIL-88B- $NH_2(Fe)$] and MIL-101- $NH_2(Cr)$ [Pd@MIL-101- $NH_2(Cr)$] (Figure 20).⁵¹ The TEM images revealed the existence in both MOFs of uniformly distributed Pd NPs with the average size of 2 nm. This particle size is compatible with the presumed incorporation of Pd NPs inside the pore voids of these MOFs. Powder XRD confirmed that the crystallinity of these MOFs is not disturbed during the encapsulation of Pd NPs.

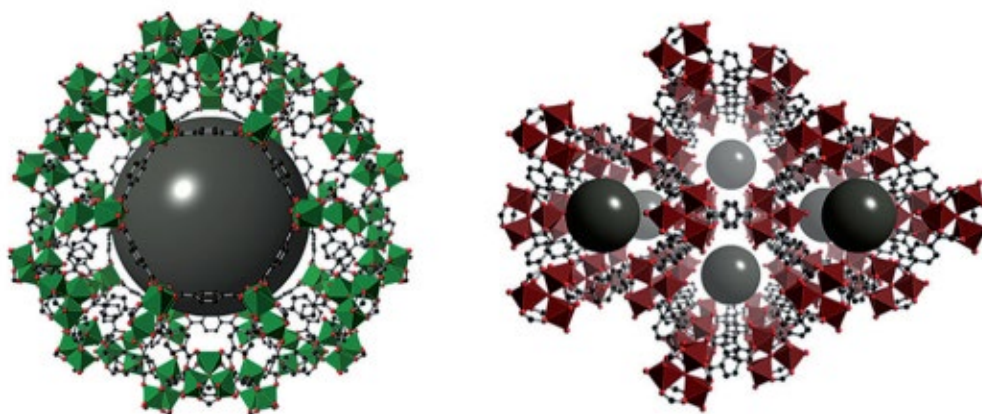
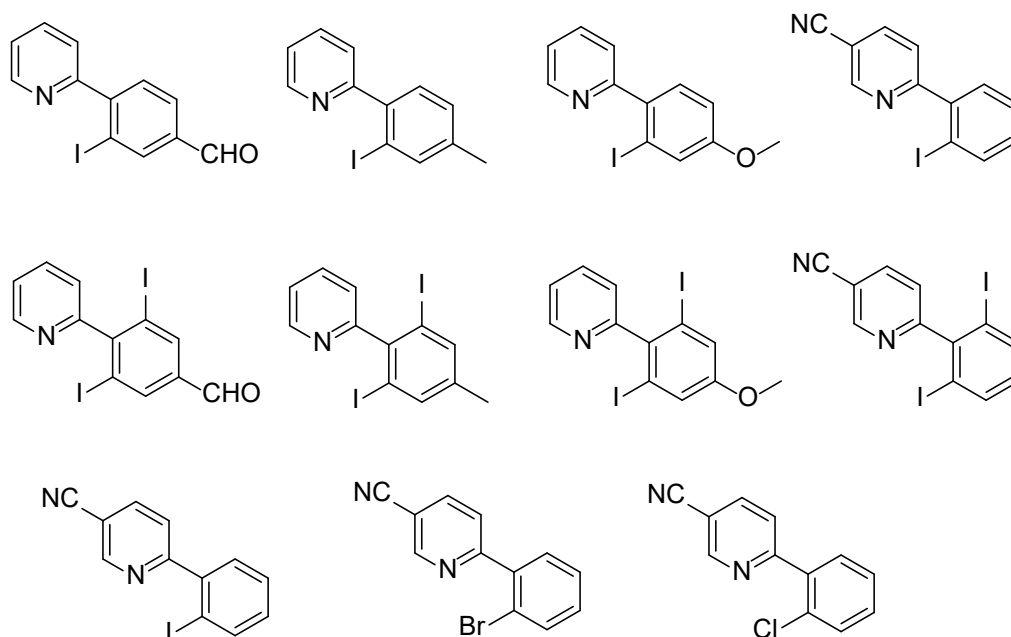


Figure 20. Pd NPs supported in MIL-101- $NH_2(Cr)$ cages (left, green) and MIL-88B- $NH_2(Fe)$ channels (right, red). Reprinted with permission from ref.51 Copyright 2016 Wiley.

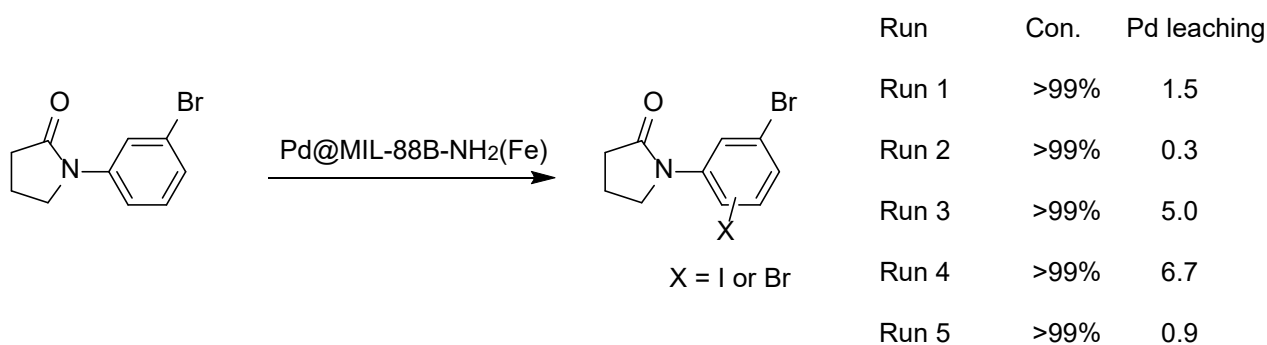
The catalytic performance of these MOFs was investigated in the halogenations of 2-phenylpyridine through C-H activation using N-iodosuccinimide as iodine source. The use of

Pd@MIL-101-NH₂(Cr) as catalyst under optimized reaction conditions afforded 74 % yield of 2-(2-iodophenyl)pyridine at 50 °C in acetic acid. In contrast, the product yield enhanced to 98 % towards 2-(2,6-diiodophenyl)pyridine using Pd@MIL-101-NH₂(Cr) catalyst at 80 °C in 1,2-dichloroethane and p-toluenesulfonic acid as additive. Similarly, Pd@MIL-88B-NH₂(Fe) also efficiently promoted the reaction to achieve 81 % yield of 2-(2-iodophenyl)pyridine at 50 °C in acetic acid. In contrast, the use of Pd/C (10 wt%) afforded only 16 % yield of 2-(2-iodophenyl)pyridine under identical conditions. These results clearly suggest that the use of MOFs as support for Pd NPs provides a convenient platform to achieve an optimal activity of Pd with minimal reactant diffusion limitations due to their large pore size. Thus, these MOF catalysts favour a high yield of the desired products. Scheme 31 shows the various halogenated compounds prepared using these catalysts.

Stability of Pd containing MOFs was established by performing reusability tests using N-(3-bromophenyl)pyrrolidin-2-one as a model substrate under the optimized reaction conditions (Scheme 32). Although both catalysts exhibited around 99 % conversion for five runs, powder XRD analysis indicated significant changes in the crystallinity of MIL-101(Cr)-NH₂. In contrast, MIL-88B-NH₂ framework retained its crystallinity, but, a shift of the peaks to lower 2θ values was, however, observed. Furthermore, TEM images of the reused sample showed considerable agglomeration of Pd NPs, thus indicating instability of catalyst.



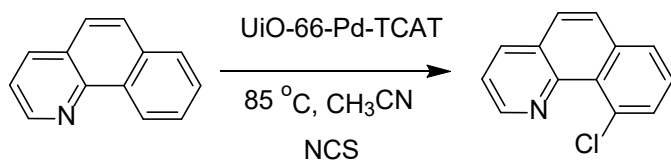
Scheme 31. Catalytic activity of Pd@MIL-88B-NH₂(Fe) and Pd@MIL-101-NH₂(Cr) MOF to promote ortho halogenations of 2-phenylpyridines.



Scheme 32. Reusability of Pd@MIL-88B-NH₂(Fe) catalyst under optimized reaction conditions.

Similarly, Cohen and co-workers have reported a convenient method for halogenation of 2-phenylpyridines with N-halosuccinimides using UiO-Pd-TCAT (see structure in Figure 21) as solid catalyst.⁵² The reaction between benzo[h]quinoline and N-chlorosuccinimide (NCS) using UiO-Pd-TCAT as catalyst achieved 95 % yield (Scheme 33) of monochlorinated benzo[h]quinoline product. In contrast, a control experiment with UiO-66-TCAT lacking Pd

showed no product formation under similar conditions. Recyclability tests indicated that the catalyst can be reused five runs without significant activity decay. This catalyst was able to promote halogenations of a series of benzo[h]quinolines and 2-phenylpyridines to their respective derivatives using in moderate to high yield.



Scheme 33. Chlorination of benzo[h]quinoline catalyzed by UiO-66-Pd-TCAT.

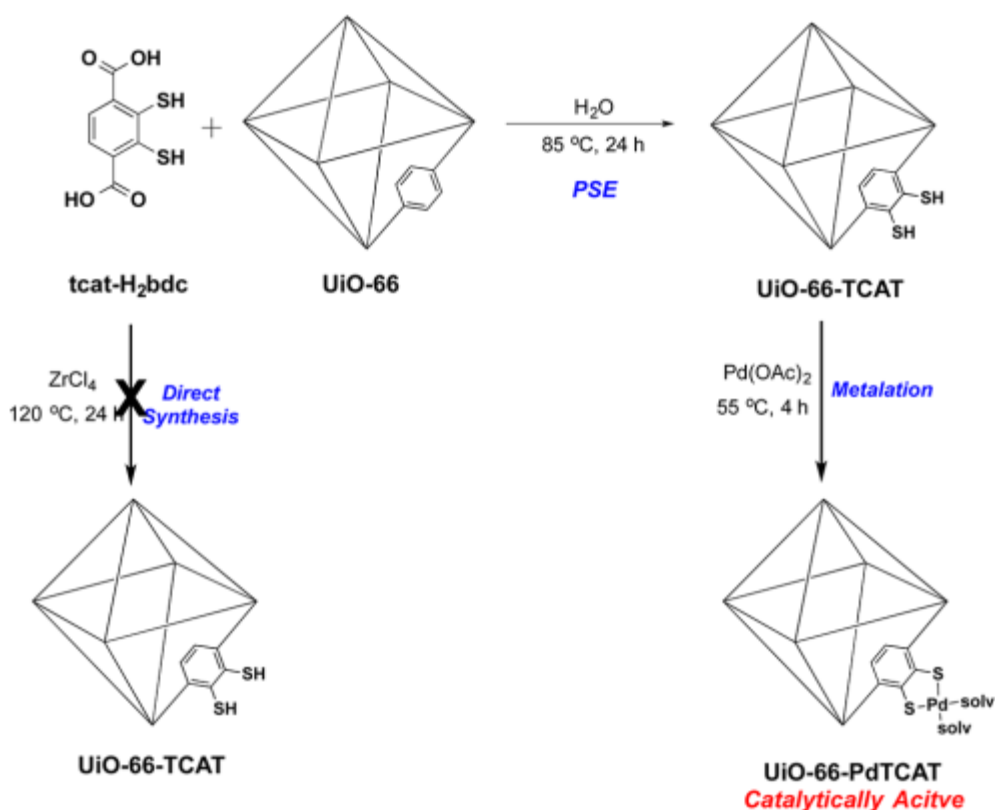


Figure 21. Synthesis of UiO-66-TCAT and UiO-66-PdTCAT. Reprinted with permission from ref.52 Copyright 2015 American Chemical Society.

Recently, a porphyrin MOF, namely PCN-602, was synthesized (Figure 22) by reacting a 12-connected $[\text{Ni}_8(\text{OH})_4(\text{H}_2\text{O})_2\text{Pz}_{12}]$ (Pz = pyrazolate) cluster and a

pyrazolate-based porphyrin ligand, 5,10,15,20-tetrakis(4-(pyrazolate-4-yl)-phenyl)porphyrin. The structure of PCN-602 possesses a larger window size of 6.3x14.2 Å whereas PCN-601 has much smaller window size, around 2.1x8.0 Å. The catalytic activity of PCN-602 was studied for the C-H halogenation of cycloalkanes.⁵³ The activity of PCN-602 was examined in the chlorination of cyclohexane using NaClO and tetrabutylammonium chloride in dichloromethane at room temperature, whereby 92 % of chlorocyclohexane yield was achieved (Scheme 34). In contrast, this reaction exhibited only 57 % yield with Mn(TPP)Cl (H₂TPP = meso-tetraphenylporphyrin) under identical conditions. The enhanced activity shown by PCN-602 is due to its porous and rigid structure, while the homogeneous catalyst undergoes fast dimerization that causes the loss of its active centres.

To develop an environmentally more benign procedure avoiding dichloromethane a series of control experiments using other solvents were carried out. A yield of 93 % of chlorocyclohexane was achieved at room temperature in acetone. In comparison, the use of Mn(TPP)Cl as homogeneous catalyst exhibited only 8 % yield under identical conditions, which again indicates the superior performance of PCN-602. On the other hand, PCN-601(Mn) was employed as catalyst for cyclohexane chlorination, reaching 15 % yield under identical conditions. This inferior activity of PCN-601(Mn) is ascribed to diffusion limitations experienced by substrates and reagents through the smaller pore windows of PCN-601(Mn) compared to PCN-602(Mn) MOF. PCN-602(Mn) exhibited high activity after three consecutive cycles, giving 92 % yield. The structural integrity of the recycled PCN-602 was confirmed by powder XRD pattern and isothermal gas adsorption measurements.

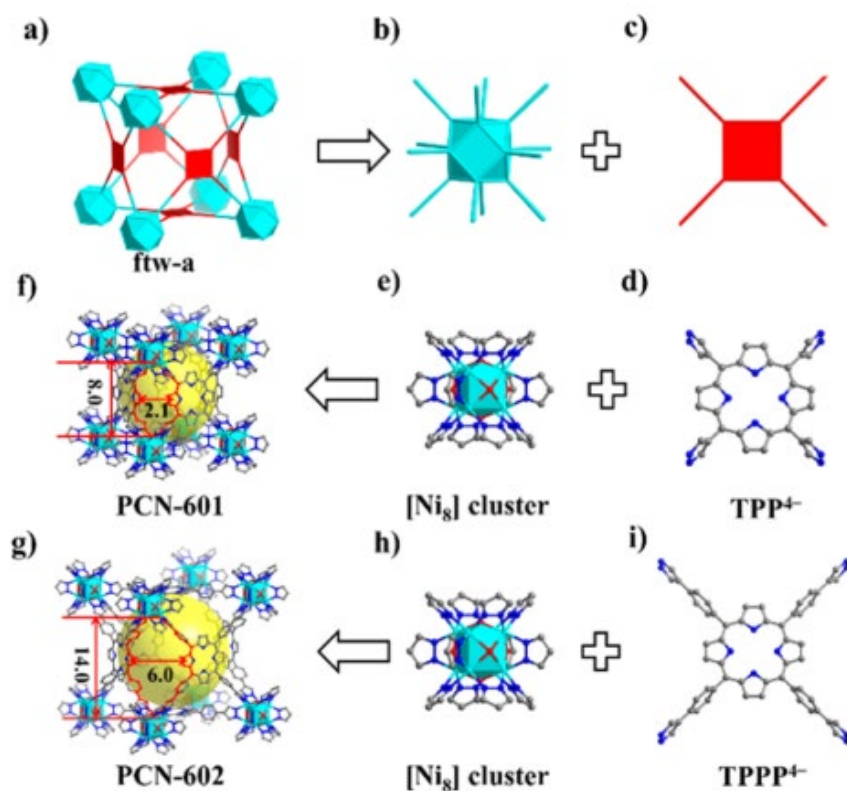
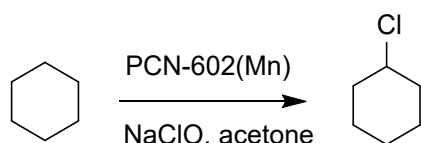


Figure 22. Reticular design and structure of PCN-602: (a) ftw-a topological net; (b) 12-connected node with O_h symmetry; (c) 4-connected node with D_{4h} symmetry; (d) TPP^4 ligand; (e and h) $[Ni_8]$ cluster; (f) structure of PCN-601 (Ni atoms in the porphyrin center are omitted for clarity); (g) proposed structure of PCN-602; and (i) $TPPP^4$ ligand. Reprinted with permission from ref.53 Copyright 2017 American Chemical Society.



Scheme 34. Conversion of cyclohexane to chlorocyclohexane catalyzed by PCN-602(Mn) using NaClO as oxidant.

7. Conclusions

Considering the importance of cross coupling reactions in current organic synthesis and the obvious advantages in terms of availability and simplicity of reagents using C-H activation, it can be expected that the importance and types of cross coupling reactions based on C-H activation will grow in the coming years. The present review has shown that due to the presence of metals with coordinatively unsaturated positions or to the presence of structural defects, MOFs are general catalysts for these types of reactions. Depending on the reaction mechanism, the catalytic centre may involve Lewis acidity or oxidizing sites and transition metal ions in MOFs exhibit general activity for both reaction types. In addition, MOFs are also suitable supports to encapsulate small size metal nanoparticles with catalytic activity in promoting C-H activation.

In the current state of the art, there is a prevalence of MOFs catalysts based on Cu over other transition metals. However, it is well known that Cu MOFs are not among the most stable materials, and therefore, it is still of interest to develop novel MOFs of metal ions of higher Coulombic charge for which the structural stability is much higher. Also, in some other cases, the active sites are noble metals as NPs or complexes. Again, it can be anticipated that noble metals will be replaced in future catalysts for more abundant and affordable metals.

Concerning the oxidative coupling, the general tendency should be to use oxygen or air as reagents. Alternatively organic hydroperoxides are considered also green oxidizing reagents to promote oxidative coupling, particularly compared to halonium ions or oxidizing reagents containing other elements that after the reaction form by-products.

In any case, it can be anticipated that the field will grow in the near future and the impact in these reactions in organic synthesis will increase also, MOFs appearing as general solid catalysts for these reactions. The final goal will be to develop general methodologies to couple two C-H bonds to form C-C and C-Y bonds with some catalytic process resulting in

high yields and wide scope from the substrate point of view due to the mild reaction conditions and the absence of corrosive reagents. It can be expected that versatility in the composition and design in MOFs will make these materials also suitable heterogeneous catalysts for these hypothetical coupling processes.

Acknowledgements

AD thanks the University Grants Commission, New Delhi, for the award of an Assistant Professorship under its Faculty Recharge Programme. AD also thanks the Department of Science and Technology, India, for the financial support through Extra Mural Research Funding (EMR/2016/006500). Financial support by the Spanish Ministry of Economy and Competitiveness (Severo Ochoa and CTQ2015-69153-CO2-1) and Generalitat Valenciana (Prometeo 2017-083) is gratefully acknowledged.

Conflict of Interest

Authors declare no conflict of interest

References

1. Li, H.; Johansson Seechurn, C. C. C.; Colacot, T. J., Development of Preformed Pd Catalysts for Cross-Coupling Reactions, Beyond the 2010 Nobel Prize. *ACS Catal.* **2012**, *2*, 1147-1164.
2. Diederich, F.; Stang, P. J., Eds. *Metal-Catalyzed Cross-Coupling Reactions*, Wiley-VCH, Weinheim, 1998.
3. Suzuki, A., Cross-Coupling Reactions of Organoboranes: An Easy Way to Construct C-C Bonds (Nobel Lecture). *Angew. Chem. Int. Ed.* **2011**, *50*, 6723-6737.
4. Miyaura, N.; Suzuki, A., Palladium-Catalyzed Cross-Coupling Reactions of Organoboron Compounds. *Chem. Rev.* **1995**, *95*, 2457-2483.
5. Wolfe, J. P.; Singer, R. A.; Yang, B. H.; Buchwald, S. L., Highly Active Palladium Catalysts for Suzuki Coupling Reactions. *J. Am. Chem. Soc.* **1999**, *121*, 9550-9561.
6. Zapf, A.; Ehrentraut, A.; Beller, M., A New Highly Efficient Catalyst System for the Coupling of Nonactivated and Deactivated Aryl Chlorides with Arylboronic Acids. *Angew. Chem. Int. Ed.* **2000**, *39*, 4153-4155.
7. Cahiez, G.; Moyeux, A., Cobalt-Catalyzed Cross-Coupling Reactions. *Chem. Rev.* **2010**, *110*, 1435-1462.
8. Jana, R.; Pathak, T. P.; Sigman, M. S., Advances in Transition Metal (Pd,Ni,Fe)-Catalyzed Cross-Coupling Reactions Using Alkyl-organometallics as Reaction Partners. *Chem. Rev.* **2011**, *111*, 1417-1492.

9. Cabri, W.; Candiani, I., Recent Developments and New Perspectives in the Heck Reaction. *Acc. Chem. Res.* **1995**, *28*, 2-7.
10. Chinchilla, R.; Nájera, C., Recent Advances in Sonogashira Reactions. *Chem. Soc. Rev.* **2011**, *40*, 5084-5121.
11. Sun, C.-L.; Li, B.-J.; Shi, Z.-J., Pd-Catalyzed Oxidative Coupling with Organometallic Reagents via C–H Activation. *Chem. Commun.* **2010**, *46*, 677-685.
12. Yi, H.; Zhang, G.; Wang, H.; Huang, Z.; Wang, J.; Singh, A. K.; Lei, A., Recent Advances in Radical C–H Activation/Radical Cross-Coupling. *Chem. Rev.* **2017**, *117*, 9016-9085.
13. Sheldon, R. A., Homogeneous Catalysts to Solid Catalysts. *Curr. Opin. Solid State Mater. Sci.* **1996**, *1*, 101-106.
14. Dhakshinamoorthy, A.; Opanasenko, M.; Čejka, J.; Garcia, H., Metal Organic Frameworks as Heterogeneous Catalysts for the Production of Fine Chemicals. *Catal. Sci. Technol.* **2013**, *3*, 2509-2540.
15. Zhu, L.; Liu, X.-Q.; Jiang, H.-L.; Sun, L.-B., Metal–Organic Frameworks for Heterogeneous Basic Catalysis. *Chem. Rev.* **2017**, *117*, 8129-8176.
16. Dhakshinamoorthy, A.; Li, Z.; Garcia, H., Catalysis and Photocatalysis by Metal Organic Frameworks. *Chem. Soc. Rev.* **2018**, *47*, 8134-8172
17. Stock, N.; Biswas, S., Synthesis of Metal–Organic Frameworks (MOFs): Routes to Various MOF Topologies, Morphologies, and Composites. *Chem. Rev.* **2012**, *112*, 933-969.
18. Bosch, M.; Yuan, S.; Rutledge, W.; Zhou, H.-C., Stepwise Synthesis of Metal–Organic Frameworks. *Acc. Chem. Res.* **2017**, *50* 857-865.
19. Reinsch, H.; Stock, N., Synthesis of MOFs: A Personal View on Rationalisation, Application and Exploration. *Dalton Trans.* **2017**, *46*, 8339-8349.
20. Serra-Crespo, P.; Ramos-Fernandez, E. V.; Gascon, J.; Kapteijn, F., Synthesis and Characterization of an Amino Functionalized MIL-101(Al): Separation and Catalytic Properties. *Chem. Mater.* **2011**, *23*, 2565-2572.
21. Rowsell, J. L. C.; Yaghi, O. M., Metal–Organic Frameworks: A New Class of Porous Materials. *Micropor. Mesopor. Mater.* **2004**, *73*, 3-14.
22. Li, M.; Li, D.; O’Keeffe, M.; Yaghi, O. M., Topological Analysis of Metal–Organic Frameworks with Polytopic Linkers and/or Multiple Building Units and the Minimal Transitivity Principle. *Chem. Rev.* **2014**, *114*, 1343-1370.
23. Wang, Z.; Cohen, S. M., Postsynthetic Modification of Metal–Organic Frameworks. *Chem. Soc. Rev.* **2009**, *38*, 1315-1329.
24. Tanabe, K. K.; Cohen, S. M., Postsynthetic Modification of Metal–Organic Frameworks—a Progress Report. *Chem. Soc. Rev.* **2011**, *40*, 498-519.
25. Hu, Z.; Zhao, D., Metal–Organic Frameworks with Lewis Acidity: Synthesis, Characterization, and Catalytic Applications. *CrystEngComm* **2017**, *19*, 4066-4081.
26. Sholl, D. S.; Lively, R. P., Defects in Metal–Organic Frameworks: Challenge or Opportunity? *J. Phys. Chem. Lett.* **2015**, *6*, 3437-3444.
27. Fang, Z.; Bueken, B.; De Vos, D. E.; Fischer, R. A., Defect-Engineered Metal–Organic Frameworks. *Angew. Chem. Int. Ed.* **2015** *54*, 7234-7254.
28. Dhakshinamoorthy, A.; Alvaro, M.; Garcia, H., Metal–Organic Frameworks as Heterogeneous Catalysts for Oxidation Reactions. *Catal. Sci. Technol.* **2011**, *1*, 856-867.
29. Dhakshinamoorthy, A.; Asiri, A. M.; Garcia, H., Metal–Organic Frameworks as Catalysts for Oxidation Reactions. *Chem. Eur. J.* **2016**, *22*, 8012-8024.
30. Phan, N. T. S.; Nguyen, C. K.; Nguyen, T. T.; Truong, T., Towards Applications of Metal–Organic Frameworks in Catalysis: C–H Direct Activation of Benzoxazole with Aryl Boronic Acids Using Ni₂(BDC)₂(DABCO) as an Efficient Heterogeneous Catalyst *Catal. Sci. Technol.* **2014**, *4*, 369-377.
31. Huang, C.; Wu, J.; Song, C.; Ding, R.; Qiao, Y.; Hou, H.; Chang, J.; Fan, Y., Reversible Conversion of Valence-Tautomeric Copper Metal–Organic Frameworks Dependent Single-Crystal-to-Single-Crystal Oxidation/Reduction: a Redox-Switchable Catalyst for C–H Bonds Activation Reaction. *Chem. Commun.* **2015**, *51*, 10353-10356.

32. Le, H. T. N.; Nguyen, T. T.; Vu, P. H. L.; Truong, T.; Phan, N. T. S., Ligand-Free Direct C-Arylation of Heterocycles with Aryl Halides Over a Metal-Organic Framework Cu₂(BPDC)₂(BPY) as an Efficient and Robust Heterogeneous Catalyst. *J. Mol. Catal. A: Chem.* **2014**, *391*, 74-82.
33. Huang, Y.-B.; Shen, M.; Wang, X.; Huang, P.; Chen, R.; Lin, Z.-J.; Cao, R., Water-Medium C-H Activation Over a Hydrophobic Perfluoroalkane-Decorated Metal-Organic Framework Platform. *J. Catal.* **2016**, *333*, 1-7.
34. Huang, Y.; Ma, T.; Huang, P.; Wu, D.; Lin, Z.; Cao, R., Direct C-H Bond Arylation of Indoles with Aryl Boronic Acids Catalyzed by Palladium Nanoparticles Encapsulated in Mesoporous Metal-Organic Framework. *ChemCatChem* **2013**, *5*, 1877-1883.
35. Park, T.-H.; Hickman, A. J.; Koh, K.; Martin, S.; Wong-Foy, A. G.; Sanford, M. S.; Matzger, A. J., Highly Dispersed Palladium(II) in a Defective Metal-Organic Framework: Application to C-H Activation and Functionalization. *J. Am. Chem. Soc.* **2011**, *133*, 20138-20141.
36. Pham, P. H.; Doan, S. H.; Tran, H. T. T.; Nguyen, N. N.; Phan, A. N. Q.; Le, H. V.; Tu, T. N.; Phan, N. T. S., A New Transformation of Coumarins via Direct C-H Bond Activation Utilizing an Iron-Organic Framework as a Recyclable Catalyst. *Catal. Sci. Technol.* **2018**, *8*, 1267-1271
37. Dang, H. T.; Lieu, T. N.; Truong, T.; Phan, N. T. S., Direct Alkenylation of 2-Substituted Azaarenes with Carbonyls via CH Bond Activation Using Iron-Based Metal-Organic Framework Fe₃O(BPDC)₃ as an Efficient Heterogeneous Catalyst. *J. Mol. Catal. A: Chem.* **2016**, *420*, 237-245.
38. Fei, H.; Cohen, S. M., A Robust, Catalytic Metal-Organic Framework with Open 2,2'-Bipyridine Sites. *Chem. Commun.* **2014**, *50*, 4810-4812.
39. Chen, L.; Rangan, S.; Li, J.; Jiang, H.; Li, Y., A Molecular Pd(II) Complex Incorporated into a MOF as a Highly Active Single-Site Heterogeneous Catalyst for C-Cl Bond Activation. *Green Chem.* **2014**, *16*, 3978-3985.
40. Sun, R.; Liu, B.; Li, B.-G.; Jie, S., Palladium(II)@Zirconium-Based Mixed-Linker Metal-Organic Frameworks as Highly Efficient and Recyclable Catalysts for Suzuki and Heck Cross-Coupling Reactions. *ChemCatChem* **2016**, *8*, 3261-3271.
41. Tran, N. T. T.; Tran, Q. H.; Truong, T., Removable Bidentate Directing Group Assisted-Recyclable Metal-Organic Frameworks-Catalyzed Direct Oxidative Amination of Sp² C-H Bonds. *J. Catal.* **2014**, *320*, 9-15.
42. Hoang, T. T.; To, T. A.; Cao, V. T. T.; Nguyen, A. T.; Nguyen, T. T.; Phan, N. T. S., Direct Oxidative C-H Amination of Quinoxalinones Under Copper-Organic Framework Catalysis. *Catal. Commun.* **2017**, *101*, 20-25.
43. Xu, F.; Kang, W.-F.; Wang, X.-N.; Kou, H.-D.; Jin, Z.; Liu, C.-S., Synergic Effect of Copper-Based Metal-Organic Frameworks for Highly Efficient C-H Activation of Amidines. *RSC Adv.* **2017**, *7*, 51658-51662.
44. Tran, T. V.; Le, H. T. N.; Ha, H. Q.; Duong, X. N. T.; Nguyen, L. H. T.; Doan, T. L. H.; Nguyen, H. L.; Truong, T., A Five Coordination Cu(II) Cluster-Based MOF and its Application in the Synthesis of Pharmaceuticals via sp³ C-H/N-H Oxidative Coupling. *Catal. Sci. Technol.* **2017**, *7*, 3453-3458.
45. Wang, L.; Agnew, D. W.; Yu, X.; Figueroa, J. S.; Cohen, S. M., A Metal-Organic Framework with Exceptional Activity for C-H Bond Amination. *Angew. Chem. Int. Ed.* **2018**, *57*, 511-515.
46. Thacker, N. C.; Lin, Z.; Zhang, T.; Gilhula, J. C.; Abney, C. W.; Lin, W., Robust and Porous β-Diketimate-Functionalized Metal-Organic Frameworks for Earth-Abundant-Metal-Catalyzed C-H Amination and Hydrogenation. *J. Am. Chem. Soc.* **2016**, *138*, 3501-3509.
47. Phan, N. T. S.; Vu, P. H. L.; Nguyen, T. T., Expanding Applications of Copper-Based Metal-Organic Frameworks in Catalysis: Oxidative C-O Coupling by Direct C-H Activation of Ethers over Cu₂(BPDC)₂(BPY) as an Efficient Heterogeneous Catalyst. *J. Catal.* **2013**, *306*, 38-46.
48. Xiao, D. J.; Bloch, E. D.; Mason, J. A.; Queen, W. L.; Hudson, M. R.; Planas, N.; Borycz, J.; Dzubak, A. L.; Verma, P.; Lee, K.; Bonino, F.; Crocella, V.; Yano, J.; Bordiga, S.; Truhlar, D. G.; Gagliardi, L.; Brown, C. M.; Long, J. R., Oxidation of Ethane to Ethanol by N₂O in a Metal-Organic Framework with Coordinatively Unsaturated Iron(II) Sites. *Nature Chem.* **2014**, *6*, 590-595.

49. Manna, K.; Zhang, T.; Greene, F. X.; Lin, W., Bipyridine- and Phenanthroline-Based Metal–Organic Frameworks for Highly Efficient and Tandem Catalytic Organic Transformations via Directed C–H Activation. *J. Am. Chem. Soc.* **2015**, *137*, 2665–2673.
50. Lin, Z.; Thacker, N. C.; Sawano, T.; Drake, T.; Ji, P.; Lan, G.; Cao, L.; Liu, S.; Wang, C.; Lin, W., Metal–Organic Layers Stabilize Earth-Abundant Metal–Terpyridine Diradical Complexes for Catalytic C–H Activation. *Chem. Sci.* **2018**, *9*, 143–151.
51. Pascanu, V.; Carson, F.; Vico Solano, M.; Su, J.; Zou, X.; Johansson, M. J.; Martin-Matute, B., Selective Heterogeneous C–H Activation/Halogenation Reactions Catalyzed by Pd@MOF Nanocomposites. *Chem. Eur. J.* **2016**, *22*, 3729–3737.
52. Fei, H.; Cohen, S. M., Metalation of a Thiocatechol-Functionalized Zr(IV)-Based Metal–Organic Framework for Selective C–H Functionalization. *J. Am. Chem. Soc.* **2015**, *137*, 2191–2194.
53. Lv, X.-L.; Wang, K.; Wang, B.; Su, J.; Zou, X.; Xie, Y.; Li, J.-R.; Zhou, H.-C., A Base-Resistant Metalloporphyrin Metal–Organic Framework for C–H Bond Halogenation. *J. Am. Chem. Soc.* **2017**, *139*, 211–217.
54. Huang, C.; Gevorgyan, V., TBDPS and Br-TBDPS Protecting Groups as Efficient Aryl Group Donors in Pd-Catalyzed Arylation of Phenols and Anilines. *J. Am. Chem. Soc.* **2009**, *131*, 10844–10845.
55. Do, H.-Q.; Daugulis, O., Copper-Catalyzed Arylation and Alkenylation of Polyfluoroarene C–H Bonds. *J. Am. Chem. Soc.* **2008**, *130*, 1128–1129.
56. Tan, K.; Nijem, N.; Canepa, P.; Gong, Q.; Li, J.; Thonhauser, T.; Chabal, Y. J., Stability and Hydrolyzation of Metal Organic Frameworks with Paddle-Wheel SBUs upon Hydration. *Chem. Mater.* **2012**, *24* 3153–3167.
57. Pichon, A.; Fierro, C. M.; Nieuwenhuyzen, M.; James, S. L., A Pillared-Grid MOF with Large Pores Based on the Cu₂(O₂CR)₄ Paddle-Wheel. *CrystEngComm* **2007**, *9*, 449–451.
58. Luz, I.; Llabrés i Xamena, F. X.; Corma, A., Bridging Homogeneous and Heterogeneous Catalysis with MOFs: Cu-MOFs as Solid Catalysts for Three-Component Coupling and Cyclization Reactions for the Synthesis of Propargylamines, Indoles and Imidazopyridines. *J. Catal.* **2012**, *285*, 285–291.
59. Férey, G.; Mellot-Draznieks, C.; Serre, C.; Millange, F.; Dutour, J.; Surble, S.; Margiolaki, I., A Chromium Terephthalate-Based Solid with Unusually Large Pore Volumes and Surface Area. *Science* **2005**, *309*, 2040–2042.
60. Dan-Hardi, M.; Chevreau, H.; Devic, T.; Horcajada, P.; Maurin, G.; Férey, G.; Popov, D.; Riekell, C.; Wuttke, S.; Lavalley, J.-C.; Vimont, A.; Boudewijns, t.; De Vos, D. E.; Serre, C., How Interpenetration Ensures Rigidity and Permanent Porosity in a Highly Flexible Hybrid Solid. *Chem. Mater.* **2012**, *24* 2486–2492.
61. Weck, M.; Jones, C. W., Mizoroki–Heck Coupling Using Immobilized Molecular Precatalysts: Leaching Active Species from Pd Pincers, Entrapped Pd Salts, and Pd NHC Complexes. *Inorg. Chem.* **2007**, *46*, 1865–1875.
62. Yuan, B.; Pan, Y.; Li, Y.; Yin, B.; Jiang, H., A Highly Active Heterogeneous Palladium Catalyst for the Suzuki–Miyaura and Ullmann Coupling Reactions of Aryl Chlorides in Aqueous Media *Angew. Chem. Int. Ed.* **2010**, *49*, 4054–4058.
63. Elumalai, P.; Mamlouk, H.; Yiming, W.; Feng, L.; Yuan, S.; Zhou, H.-C.; Madrahimov, S. T., Recyclable and Reusable Heteroleptic Nickel Catalyst Immobilized on Metal–Organic Framework for Suzuki–Miyaura Coupling. *ACS Appl. Mater. Interfaces* **2018**, *10* 41431–41438.
64. Dhakshinamoorthy, A.; Asiri, A. M.; Garcia, H., Metal–Organic Frameworks Catalyzed C–C and C–Heteroatom Coupling Reactions. *Chem. Soc. Rev.* **2015**, *44*, 1922–1947
65. Collet, F.; Lescot, C.; Dauban, P., Catalytic C–H Amination: The Stereoselectivity Issue. *Chem. Soc. Rev.* **2011**, *40*, 1926–1936.
66. Roizen, J. L.; Harvey, M. E.; Du Bois, J., Metal-Catalyzed Nitrogen-Atom Transfer Methods for the Oxidation of Aliphatic C–H Bonds. *Acc. Chem. Res.* **2012**, *45*, 911–922.
67. Ramirez, T. A.; Zhao, B.; Shi, Y., Recent Advances in Transition Metal-Catalyzed sp³ C–H Amination Adjacent to Double Bonds and Carbonyl Groups. *Chem. Soc. Rev.* **2012**, *41*, 931–942.

68. Zhao, Y. S. H.; Weiping, S., Rhodium(III)-Catalyzed Intermolecular N-Chelator-Directed Aromatic C–H Amidation with Amides. *Org. Lett.* **2013**, *15*, 5106-5109.
69. Yoo, E. J.; Ma, S.; Mei, T.-S.; Chan, K. S. L.; Yu, J.-Q., Pd-Catalyzed Intermolecular C–H Amination with Alkylamines. *J. Am. Chem. Soc.* **2011**, *133*, 7652-7655.
70. Taylor, A. P.; Robinson, R. P.; Fobian, Y. M.; Blakemore, D. C.; Jones, L. H.; Fadeyi, O., Modern Advances in Heterocyclic Chemistry in Drug Discovery. *Org. Biomol. Chem.* **2016**, *14*, 6611-6637.
71. Mamedov, V. A., Recent Advances in the Synthesis of Benzimidazol(on)es via Rearrangements of Quinoxalin(on)es. *RSC Adv.* **2016**, *6*, 42132-42172.
72. Wiethan, C.; Franceschini, S. Z.; Bonacorso, H. G.; Stradiotto, M., Synthesis of Pyrazolo[1,5-a]quinoxalin-4(5H)-ones via One-Pot Amidation/N-Arylation Reactions Under Transition Metal-Free Conditions. *Org. Biomol. Chem.* **2016**, *14*, 8721-8727.
73. Katz, M. J.; Howarth, A. J.; Moghadam, P. Z.; DeCoste, J. B.; Snurr, R. Q.; Hupp, J. T.; Farha, O. K., High Volumetric Uptake of Ammonia Using Cu-MOF-74/Cu-CPO-27. *Dalton Trans.* **2016**, *45*, 4150-4153.
74. Sanz, R.; Martínez, F.; Orcajo, G.; Wojtas, L.; Briones, D., Synthesis of a Honeycomb-Like Cu-Based Metal–Organic Framework and its Carbon Dioxide Adsorption Behaviour. *Dalton Trans.* **2013**, *42* 2392-2398.
75. Dhakshinamoorthy, A.; Asiri, A. M.; Concepcion, P.; Garcia, H., Synthesis of Borasiloxanes by Oxidative Hydrolysis of Silanes and Pinacolborane using Cu₃(BTC)₂ as a Solid Catalyst. *Chem. Commun.* **2017**, *53*, 9998-10001.
76. Perez-Mayoral, E.; Cejka, J., [Cu₃(BTC)₂]: A Metal–Organic Framework Catalyst for the Friedländer Reaction. *ChemCatChem* **2011**, *3*, 157-159.
77. Tranchemontagne, D. J.; Mendoza-Cortes, J. L.; O'Keeffe, M.; Yaghi, O. M., Secondary Building Units, Nets and Bonding in the Chemistry of Metal–Organic Frameworks. *Chem. Soc. Rev.* **2009**, *38*, 1257-1283.
78. Bosch, M.; Zhang, M.; Zhou, H.-C., Increasing the Stability of Metal-Organic Frameworks. *Adv. Chem.* **2014**, 182327.
79. Dhakshinamoorthy, A.; Alvaro, M.; Concepcion, P.; Garcia, H., Chemical Instability of Cu₃(BTC)₂ by Reaction with Thiols. *Catal. Commun.* **2011**, *12*, 1018-1021.
80. Wang, L.; Morales, J.; Wu, T.; Zhao, X.; Beyermann, W. P.; Bu, X. H.; Feng, P. Y., Assembly of Super-Supertetrahedral Metal–Organic Clusters into a Hierarchical Porous Cubic Framework. *Chem. Commun.* **2012**, *48*, 7498-7500.
81. Bourget-Merle, L.; Lappert, M. F.; Severn, J. R., The Chemistry of β -Diketiminatometal Complexes. *Chem. Rev.* **2002**, *102*, 3031–3066.
82. Evano, G.; Blanchard, N.; Toumi, M., Copper-Mediated Coupling Reactions and Their Applications in Natural Products and Designed Biomolecules Synthesis. *Chem. Rev.* **2008**, *108*, 3054-3131.
83. Würtz, S.; Glorius, F., Surveying Sterically Demanding N-Heterocyclic Carbene Ligands with Restricted Flexibility for Palladium-catalyzed Cross-Coupling Reactions. *Acc. Chem. Res.* **2008**, *41*, 1523-1533.
84. Rudolph, A.; Lautens, M., Secondary Alkyl Halides in Transition-Metal-Catalyzed Cross-Coupling Reactions. *Angew. Chem. Int. Ed.* **2009**, *48*, 2656-2670.
85. Stuart, D. R.; Fagnou, K., The Catalytic Cross-Coupling of Unactivated Arenes. *Science* **2007**, *316*, 1172-1175.
86. Verma, P.; Vogiatzis, K. D.; Planas, N.; Borycz, J.; Xiao, D. J.; Long, J. R.; Gagliardi, L.; Truhlar, D. G., Mechanism of Oxidation of Ethane to Ethanol at Iron(IV)–Oxo Sites in Magnesium-Diluted Fe₂(dobdc). *J. Am. Chem. Soc.* **2015**, *137*, 5770–5781.
87. Manna, K.; Ji, P.; Lin, Z.; Greene, F. X.; Urban, A.; Thacker, N. C.; Lin, W., Chemoselective Single-Site Earth-Abundant Metal Catalysts at Metal–Organic Framework Nodes. *Nat. Commun.* **2016**, *7*, 12610.

88. Furukawa, T.; Tobisu, M.; Chatani, N., Nickel-Catalyzed Borylation of Arenes and Indoles via C–H Bond Cleavage. *Chem. Commun.* **2015**, *51*, 6508-6511.
89. Shimada, S.; Batsanov, A. S.; Howard, J. A. K.; Marder, T. B., Formation of Aryl- and Benzylboronate Esters by Rhodium-Catalyzed C-H Bond Functionalization with Pinacolborane. *Angew. Chem. Int. Ed.* **2001**, *40*, 2168-2171.
90. Cao, L.; Lin, Z.; Peng, F.; Wang, W.; Huang, R.; Wang, C.; Yan, J.; Liang, J.; Zhang, Z.; Zhang, T.; Long, L.; Sun, J.; Lin, W., Self-Supporting Metal-Organic Layers as Single-Site Solid Catalysts. *Angew. Chem. Int. Ed.* **2016**, *55*, 4962-4966.

For Table of Contents Only

